

South Dakota State University

Open PRAIRIE: Open Public Research Access Institutional Repository and Information Exchange

Electronic Theses and Dissertations

2019

Coordinated Smart Home Thermal and Energy Management System Using a Co-simulation Framework

Prateek Munankarmi

South Dakota State University

Follow this and additional works at: <https://openprairie.sdstate.edu/etd>



Part of the [Controls and Control Theory Commons](#), and the [Systems and Communications Commons](#)

Recommended Citation

Munankarmi, Prateek, "Coordinated Smart Home Thermal and Energy Management System Using a Co-simulation Framework" (2019). *Electronic Theses and Dissertations*. 3163.
<https://openprairie.sdstate.edu/etd/3163>

This Thesis - Open Access is brought to you for free and open access by Open PRAIRIE: Open Public Research Access Institutional Repository and Information Exchange. It has been accepted for inclusion in Electronic Theses and Dissertations by an authorized administrator of Open PRAIRIE: Open Public Research Access Institutional Repository and Information Exchange. For more information, please contact michael.biondo@sdstate.edu.

COORDINATED SMART HOME THERMAL AND ENERGY MANAGEMENT
SYSTEM USING A CO-SIMULATION FRAMEWORK

BY

PRATEEK MUNANKARMI

A thesis submitted in partial fulfillment of the requirements for the

Master of Science

Major in Electrical Engineering

South Dakota State University

2019

COORDINATED SMART HOME THERMAL AND ENERGY MANAGEMENT
SYSTEM USING A CO-SIMULATION FRAMEWORK

PRATEEK MUNANKARMI

This thesis is approved as a creditable and independent investigation by a candidate for the Master of Science in Electrical Engineering degree and is acceptable for meeting the thesis requirements for this degree. Acceptance of this thesis does not imply that the conclusions reached by the candidates are necessarily the conclusions of the major department.

Timothy M. Hansen, Ph.D.

Thesis Advisor

Date

Robert Fourny, Ph.D.

Thesis Advisor

Date

George Hamer, Ph.D.

Acting Department Head,

Electrical Engineering and Computer Science

Date

Dean, Graduate School

Date

ACKNOWLEDGEMENTS

First and foremost, I would like to express my sincere gratitude towards my thesis advisors Dr. Timothy M. Hansen and Dr. Robert Fourney for their support and guidance throughout my research. It has been a great honor to work under the supervision of Dr. Hansen and Dr. Fourney. I would also like to thank Dr. Zhen Ni for his advice and motivation while working in the collaborative project.

Furthermore, I express special thanks to Priti Paudyal for her support, positive energy, and technical feedbacks. It was my pleasure to work in a collaborative project with Priti. I would like to thank Venkat Durvasulu, Rupak Mahat, Ujjwol Tamrakar, and Kapil Duwadi for their useful suggestions and assistance. I am also grateful to Jyotshana Paudyal and Anuj Shrestha for their support and inspirations.

Nonetheless, I am thankful to my parents Prakash Munankarmi and Ira Munankarmi, my brother Pranab Munankarmi for their encouragement and invaluable moral support during my study and research.

CONTENTS

ABBREVIATIONS	vii
LIST OF FIGURES	viii
ABSTRACT	xi
CHAPTER 1 INTRODUCTION	1
1.1 Background	1
1.2 Objective	5
1.3 Contributions	5
1.4 Thesis outline	6
CHAPTER 2 CO-SIMULATION INTERFACE BETWEEN GRIDLAB-D AND ENERGYPLUS	7
2.1 Introduction	7
2.2 Related works	8
2.3 Proposed work	9
2.4 EnergyPlus and GridLAB-D House Models	10
2.5 HEMS+ Co-Simulation Framework	12
2.6 Simulation Setup	16
2.7 Results and Discussion	20
2.8 Conclusion	22

CHAPTER 3 SMART HOME ENERGY MANAGEMENT SYSTEM IN THE CO-

SIMULATION FRAMEWORK	24
3.1 Background	24
3.2 Related works	25
3.3 Proposed work	27
3.4 Model Description	27
3.4.1 House Model	28
3.4.2 HVAC Model	28
3.4.3 Appliance Model	31
3.5 Description of HEMS framework	31
3.5.1 Co-simulation Framework	32
3.5.2 HEMS optimization	32
3.5.3 Model predictive control	35
3.5.4 Overall algorithm	36
3.6 Simulation Setup	37
3.7 Results and Discussion	40
3.7.1 Winter Months	40
3.7.2 Summer Months	45
3.8 Conclusion	46

CHAPTER 4 HIERARCHICAL CONTROL FRAMEWORK WITH NOVEL BID-

DING SCHEME FOR RESIDENTIAL COMMUNITY ENERGY

OPTIMIZATION	48
------------------------	----

4.1	Background	48
4.2	Related works	49
4.3	Proposed Work	52
4.4	Appliance Model	52
4.4.1	Air Conditioner Model	53
4.4.2	Electric Water Heater Model	54
4.4.3	Consumer Preferences and Comfort Indicator	54
4.5	Hierarchical Control Framework	56
4.5.1	Novel Continuous Reward Structure	57
4.5.2	Residential Community	59
4.5.3	Local Controller Design	59
4.5.4	Central Controller Design	61
4.5.5	Impacts on Electricity Market	63
4.6	Simulation Setup	64
4.7	Result and Discussion	67
4.8	Conclusion	72
	CHAPTER 5 CONCLUSIONS	74
	REFERENCES	76

ABBREVIATIONS

BCVTB	building controls virtual test bed
CC	central controller
CI	comfort indicator
CPP	critical peak price
DR	demand response
DRP	demand response potential
EMC	energy management controller
EV	electric vehicle
EWB	electric water heater
EWB	electric water heater
HEMS	home energy management system
HVAC	Heating Ventilation and Air Conditioning
LC	local controller
LMP	locational marginal price
MILP	mixed integer linear programming
OPF	optimal power flow
PV	photo-voltaic
RTP	real-time price
TCL	thermostatically controlled load
TOU	time of use

LIST OF FIGURES

Figure 2.1.	EnergyPlus house model developed in BEopt.	11
Figure 2.2.	Block diagram of co-simulation framework.	13
Figure 2.3.	Pseudocode for HEMS+ interface.	14
Figure 2.4.	Pseudocode for co-simulation framework.	16
Figure 2.5.	Co-simulation case study setup. HEMS controls HVAC system of house and sends the setpoint temperature to EnergyPlus. Accumulator gathers the total house consumption to send to GridLAB-D.	17
Figure 2.6.	(a) Setpoint temperature for House 1 on Jan. 9, 2017. The room temperature (solid black curve) follows optimal setpoint temperature (solid blue line) in the optimized case. The maximum and minimum allowable setpoint temperature is represented by the solid red line. (b) The comparison between substation power for base (solid red curve) and optimized case (solid blue curve). The RTP is represented by the solid green curve.	21
Figure 2.7.	Comparison between substation power for base (solid red curve) and optimized (solid blue curve) cases for Jan. 21.	22
Figure 3.1.	Comparison of power consumption of HVAC models with EnergyPlus. The HVAC model with heat gain (solid green curve) estimate the energy required by HVAC to maintain setpoint temperature accurately compared to HVAC model without heat gain (solid red curve)	30

Figure 3.2.	A system block diagram of the proposed HEMS. HEMS optimization calculates the optimized HVAC setpoint and appliance schedule and sends the optimal schedule to building model in EnergyPlus using HEMS+. The detailed EnergyPlus building model calculates the total power consumption of the house.	32
Figure 3.3.	An example of ComEd residential time-varying tariff [45].	36
Figure 3.4.	Comparison of total savings of the different months for each cases. . .	42
Figure 3.5.	HVAC, appliance, and total house power for each case on January 7, 2014. Each subplot represents the total house power for different cases for the particular day. The solid green curve represents RTP price and solid light blue curve represents DAP price in each subplot.	43
Figure 3.6.	Comparison of the room temperature and setpoint for Case-III and Case-IV for January 7, 2014.	45
Figure 4.1.	System block diagram of the proposed hierarchical control structure for residential community energy optimization. It shows the components of the proposed hierarchical framework, along with the information exchange between the components, represented by arrows.	57
Figure 4.2.	RBTS system with the location of the loads and maximum generation limits of the system [82].	65
Figure 4.3.	Total utility savings from demand reduction in each hour. The blue bar graph depicts the total utility saving each hour from the peak demand reduction, which is shown by the red curve.	67

Figure 4.4.	Normal load profiles for AC and EWH load, baseload, and total load. The one-hour interval within the black dashed rectangle represents the demand reduction period.	68
Figure 4.5.	An example of different bids submitted by LC-2. The blue dots represent the reward calculated by LC-2 for different peak demand reductions, and the red curve represents the trendline for the reward variation with increasing demand reduction.	69
Figure 4.6.	Total utility savings before and after rewards for different demand reductions. The upper line represents the total utility savings without considering reward, and the lower line represents the net utility savings after providing the consumer reward. The blue region between the lines represents the reward provided.	70
Figure 4.7.	Load profile of the residential consumers before and after demand reduction event. The red line represents the load profile before demand reduction, and the green line represents the load profile after demand reduction.	72

ABSTRACT

COORDINATED SMART HOME THERMAL AND ENERGY MANAGEMENT
SYSTEM USING A CO-SIMULATION FRAMEWORK

PRATEEK MUNANKARMI

2019

The increasing demand for electricity especially during the peak hours threaten the grid reliability. Demand response (DR), changing the load pattern of the consumer in response to system conditions, can decrease energy consumption during periods of high wholesale market price and also maintain system reliability. Residential homes consume 38% of the total electric energy in the U.S., making them promising for DR participation. Consumers can be motivated to participate in DR programs by providing incentives (incentive-based DR), or by introducing a time-varying tariff for electricity consumption (price-based DR).

A home energy management system (HEMS), an automated system which can alter the residential consumer's energy consumption pattern based on the price of electricity or financial incentives, enables the consumers to participate in such DR programs. HEMS also should consider consumer comfort during the scheduling of the heating, ventilation, and air conditioning (HVAC) and other appliances. As internal heat gain of appliances and people have a significant effect in the HVAC energy consumption, an integrated HVAC and appliance scheduling are necessary to properly evaluate potential benefits of HEMS. This work presents the formulation of HEMS considering combined scheduling of HVAC and appliances in time-varying tariff. The HEMS also considers the consumer comfort for

the HVAC and appliances while minimizing the total electricity cost.

Similarly, the HEMS also considers the detailed building model in EnergyPlus, a building energy analysis tool, to evaluate the effectiveness of the HEMS. HEMS+, a communication interface to EnergyPlus, is designed to couple HEMS and EnergyPlus in this work. Furthermore, a co-simulation framework coupling EnergyPlus and GridLAB-D, a distribution system simulation tool, is developed. This framework enables incorporation of the controllers such as HEMS and aggregator, allowing controllers to be tested in detail in both building and power system domains.

Lack of coordination among a large number of HEMS responding to same price signal results in peak more severe than the normal operating condition. This work presents an incentive-based hierarchical control framework for coordinating and controlling a large number of residential consumers' thermostatically controlled loads (TCLs) such as HVAC and electric water heater (EWH). The potential market-level economic benefits of the residential demand reduction are also quantified.

CHAPTER 1 INTRODUCTION

1.1 Background

Generally, 20% of the power generation capacity is latently available to satisfy the peak demand which occurs only for approximately 5% of the time [1]. The power system requires a sufficient generation reserve to support the grid during the peak period occurring a few hours in a year span [2]. The increasing demand for electricity, especially during the peak hours threaten the grid reliability.

A conventional approach to these issues is to match the supply with demand at all time periods. The load demand is considered as inflexible and the utilities have to match the electricity demand to maintain the grid reliability. This necessitates significant investment in increasing the generation capacity as well as expanding the transmission lines to meet the demand. This approach is capital intensive and time-consuming. An alternative to the conventional approach is changing the load pattern of the consumer, termed as demand response (DR) . DR is defined as changing the load pattern of the consumer from their normal consumption patterns in response to system conditions to induce the decrease in energy consumption during periods of high wholesale market price and maintain system reliability [3].

There are several benefits of DR. First and foremost, the DR allows to reduce the generation capacity requirements of the system which in fact results in significant cost reduction. The reduction of the peak demand by shifting of energy consumption of the consumer enables to defer the investment in peaking plants like open cycle gas turbine plants [4]. Second, the proper implementation of DR leads to lower wholesale market

prices thus creating market-wide financial benefits [3]. In the wholesale market, the market clearing price is determined by the price of the last generation resources when supply matches the demand. During the peak demand, DR averts the necessity of using expensive peaking power plants thereby lowering the wholesale market price.

Third, DR can provide ancillary services to enhance the voltage stability of the power system [5]. Similarly, DR reduces the likelihood of the forced outages thus increasing the operational security [3]. Fourth, DR supports in increasing the penetration of renewable energy in the electric grid. The intermittent nature of renewable energy like photo-voltaic (PV) and wind requires significant reserve generation to handle the fluctuation in the generation output. DR can provide this reserve capacity through load curtailment and shifting i.e. the flexible loads can balance the renewable energy fluctuations thereby promoting the integration of renewable energy.

A financial incentive is key for encouraging the consumers' to participate in DR programs and persuade such change in consumers' electricity consumption pattern. Based on incentives offered, DR programs can be categorized into two groups namely, a) price-based DR and b) incentive-based DR. In incentive-based DR, consumers reduce their electricity consumption in response to the DR signal or according to the contractual agreement and receive a financial incentive for their participation [6], [7]. The power demand and operating state of individual devices are managed by the centralized controllers which issue control signals [2]. On the other hand, a dynamic pricing structure such as Time of Use (TOU), Real-Time price (RTP) , and critical peak price (CPP) depending on the system load is introduced in price-based DR [8]. It motivates the consumers to change the electricity consumption pattern i.e. reduce the electricity

consumption during high price period by shedding or shifting energy consumption. The customers are encouraged to individually manage their own energy consumption.

Residential consumers account for 38% of the total electricity consumption in the U.S. As a major sector for consumption of the electricity, residential sector shows significant potential for such DR programs. Manually changing the energy consumption pattern for residential consumers in response to time-varying tariff or incentive signals is cumbersome. This ultimately discourages residential consumers to participate in such DR programs. A home energy management system (HEMS) automatically changes the residential energy consumption pattern based on time-varying tariff or incentive signal. HEMS can reduce the electricity bill of the consumer while considering the comfort of the consumers.

Different HEMS algorithms for managing the residential end-uses have been proposed in the literature. A convex optimization is proposed in [9], smart scheduler in [10], mixed integer linear programming (MILP) in [11], MILP and heuristic algorithm in [12], two horizon in [13], partially observable Markov decision process (POMDP) in [14]. Similarly, different heuristic and meta-heuristics algorithms such as genetic algorithm, particle swarm optimization have been considered in [15]–[19]. However, the combined scheduling of the thermal and non-thermal appliances considering the effect of heat gain of the non-thermal appliances have not been considered in the previous literature.

The internal heat gain of the appliances affects the operation of heating, ventilation, and air conditioning (HVAC). The shifting of appliances with HEMS also shifts the heat gain of the appliances and thereby affecting the HVAC energy consumption. Therefore, determining the optimal HVAC setpoint temperature, the optimal appliance schedule, as

well as heat gain of the appliance should be considered simultaneously. Thus, during the optimal scheduling of the loads in HEMS, combined scheduling of HVAC as well as appliances incorporating the heat gain of the appliances must be considered.

Similarly, HEMS can also utilize available tools such as EnergyPlus, a building energy analysis tool, to accurately model the energy consumption of the house. EnergyPlus considers the finer details of the house model including the geometry, building material and its property, orientation, internal heat gain of the appliances, and weather. EnergyPlus also considers heat dissipated by the appliances into account for the calculation of the temperature of the house and the energy required by HVAC. This detailed thermal modeling of the building for calculation of residential energy consumption in EnergyPlus allows to properly evaluate the potential benefits of HEMS. A detailed thermal model (EnergyPlus model or reduced RC model derived from EnergyPlus model) is considered in [20]–[22] for evaluating the control algorithms designed for thermal appliance (HVAC).

A greedy optimization of large number of HEMS based on same price signals causes severe peak demand issue. As, all HEMS are scheduling their load to the low price period for their individual economic benefit, it results in higher peak demand during the low price periods. Consequently, instead of providing benefits, the lack of coordination among the residential consumers participating in DR programs further exacerbates the system reliability. Thus the coordination of large number of residential consumer loads is imperative to achieve the full potential benefits of the DR programs.

A distributed direct load control for large-scale residential demand management is proposed in [23] and a bi-level coordinated optimization strategy considering online DR

potential (DRP) is proposed in [24]. However, reward for consumer participation was not considered in [23], [24]. Similarly, a for-profit aggregator-based DR scheme for only non-thermal appliances is proposed in [25]. Authors in [26] considered consumer comfort and incentives but coordination mechanisms to address sharing of demand reduction among the aggregators were not considered. A framework incorporating all key elements such coordination of demand reduction, reward distribution, consumer comfort, analysis of market-level economic benefits, and detailed appliance models is not presented in the literature.

1.2 Objective

The primary objective of this thesis was to develop algorithms for residential energy management for DR, and tools and framework to analyze and validate the control algorithms.

1.3 Contributions

The main contributions of this thesis are:

- (a) design of a novel co-simulation framework coupling EnergyPlus, a building energy analysis tool, and GridLAB-D, a distribution system simulation and analysis tool.
- (b) combined scheduling of HVAC and appliances of the residential house using a smart HEMS in co-simulation framework.
- (c) the introduction of a novel bidding scheme to coordinate the demand reduction events in hierarchical control framework as well as quantification of market-level benefits of such demand reduction.

1.4 Thesis outline

This thesis is organized as follows. Chapter 2 describes the co-simulation framework coupling EnergyPlus and GridLAB-D. A case study is presented to demonstrate the usefulness of the co-simulation framework. Chapter 3 presents a smart HEMS in co-simulation framework. Description of the appliance models, detailed formulation of the HEMS algorithm, and overall framework with co-simulation interface with EnergyPlus are presented in this Chapter. Chapter 4 describes a hierarchical control framework for controlling and coordinating a large number of residential consumer's thermostatically controlled load (TCLs) such as air conditioner and electric water heater (EWH) . Similarly, the market-level economic benefits of the framework are also quantified. Chapter 5 presents the concluding remarks of the thesis.

CHAPTER 2 CO-SIMULATION INTERFACE BETWEEN GRIDLAB-D AND ENERGYPLUS

2.1 Introduction

Residential sector consumes 38% of the total electric energy in the U.S. [27], making them promising for DR participation. Such participation from the residential consumers can decrease the energy consumption during periods of high wholesale market price and also maintain system reliability [3]. Manual changing of the energy consumption pattern for DR programs might not be convenient for residential consumers. An automated home energy management system (HEMS) enables the residential consumers to participate in such programs. HEMS is an automated system that can alter the behavior of consumer load based on the price of electricity, or other forms of incentive. HEMS can utilize the existing building energy analysis tool to analyze the energy consumption of the residential houses; one such tool is EnergyPlus [28].

EnergyPlus is a building energy analysis tool which models detailed energy consumption in buildings. EnergyPlus considers detailed building models, weather and climate, appliance schedules, and temperature setpoints to calculate the energy consumption of the building. EnergyPlus is also suitable for multi-zone modeling of buildings (e.g., multi-unit apartments, commercial buildings) as it has various detailed HVAC models suitable for large buildings with inter-zonal heat flow. Also, EnergyPlus takes heat dissipated by the appliances of the building into account for the calculation of the temperature of the house and the energy required by HVAC. This detailed thermal modeling of the house considering various factors affecting the temperature of the house

and the HVAC power makes EnergyPlus ideal for use in HEMS.

Similarly, for the analysis of the effect of one or more HEMS in the distribution feeder, a distribution system analysis tool such as GridLAB-D can be used [29].

GridLAB-D is an open-source distribution system simulation and analysis tool developed by the U.S. Department of Energy at Pacific Northwest National Laboratory. GridLAB-D incorporates the models of distribution system components from the substation to the individual house appliances.

Existing tools for distribution systems and end consumers model their target subset of the power system well, but make a simplifying assumption when modeling other subdomains [30]. Once started, these tools only stop after completion of their run-time, which does not allow real-time interaction between the subdomains and relevant controllers. To solve these problems, a *co-simulation* platform capable of incorporating multiple tools, each modeling their subdomain in detail, as a unified simulation environment while supporting real-time interaction between tools is necessary [31]. In this chapter, a novel co-simulation framework for coupling EnergyPlus and GridLAB-D is designed, allowing HEMS controllers to be tested in detail in both the building and power system domains.

2.2 Related works

In recent years, co-simulation tools have been developed for EnergyPlus and GridLAB-D. Bus.py is a communication interface that offers dynamic interaction with GridLAB-D [32]. Similarly, Building Controls Virtual Test Bed (BCVTB) provides a co-simulation interface to EnergyPlus [33]. MLE+ is co-simulation toolbox for coupling

EnergyPlus and MATLAB/Simulink [34]. Though [33] and [34] allow co-simulation with EnergyPlus, our co-simulation framework provides the ability to co-simulate EnergyPlus, GridLAB-D, and *persistent* energy controllers. In [35], a platform to co-simulate EnergyPlus, GridLAB-D, and Matpower is provided, but the information that can be communicated is limited. A custom version of EnergyPlus is required to enable co-simulation using the platform in [35] and [36]. Currently, this custom version is significantly out of date, precluding co-simulation with recent and future versions of EnergyPlus. Our co-simulation framework uses an inbuilt external interface to EnergyPlus, and all variables can be accessed via our framework, ensuring compatibility with future versions of EnergyPlus, and modeling home energy impacts on the power system through GridLAB-D.

2.3 Proposed work

A novel co-simulation framework that interacts to couple EnergyPlus and GridLAB-D is designed and developed. For this, first, a co-simulation framework that interacts with EnergyPlus, HEMS+, is designed. Second, Bus.py is integrated into the co-simulation framework to couple with GridLAB-D, modeling building impacts on the distribution systems. Finally, the co-simulation framework using a controller (HEMS), EnergyPlus, and GridLAB-D is demonstrated. The HEMS formulated in this chapter controls only heating, ventilation and air conditioning (HVAC) for the demonstration of the co-simulation framework. Detailed formulation of HEMS is discussed in Chapter 3.

2.4 EnergyPlus and GridLAB-D House Models

This section provides the comparison of EnergyPlus and GridLAB-D house model. GridLAB-D provides a residential building model where the estimation of building heating/cooling loads are simplified as a function of lumped building parameters, weather, internal gains, and thermostat setpoints [37]. Alternatively, EnergyPlus considers the finer details of building geometry and orientation, along with internal gains and weather for estimation of heating/cooling loads. EnergyPlus is also suitable for multi-zone modeling of buildings (e.g., multi-unit apartments, commercial buildings) as it has various detailed HVAC models suitable for large buildings with inter-zonal heat flow.

For a fair comparison of GridLAB-D and EnergyPlus models, the same residential house model is considered, shown in Fig. 2.1. The parameters of the house for both EnergyPlus and GridLAB-D are presented in Table 2.1. BEopt [38], residential building energy evaluation software, is used to create the house model for EnergyPlus. The internal loads and occupancy schedules for both house models are designed according to [39]. All home appliance models are defined in GridLAB-D (using a ZIP load model) with the same internal gain as EnergyPlus so that the total internal gain of both houses remains the same for heating/cooling load calculations. The infiltration rate of the GridLAB-D model is matched to the EnergyPlus house, and the energy management system (EMS) of EnergyPlus is programmed for creating the same thermostat deadband as GridLAB-D.

The energy consumption of both house models is calculated for the month of January using the typical meteorological year (TMY3) weather format for Chicago, IL. Energy consumption of the EnergyPlus house model with an eastern orientation was

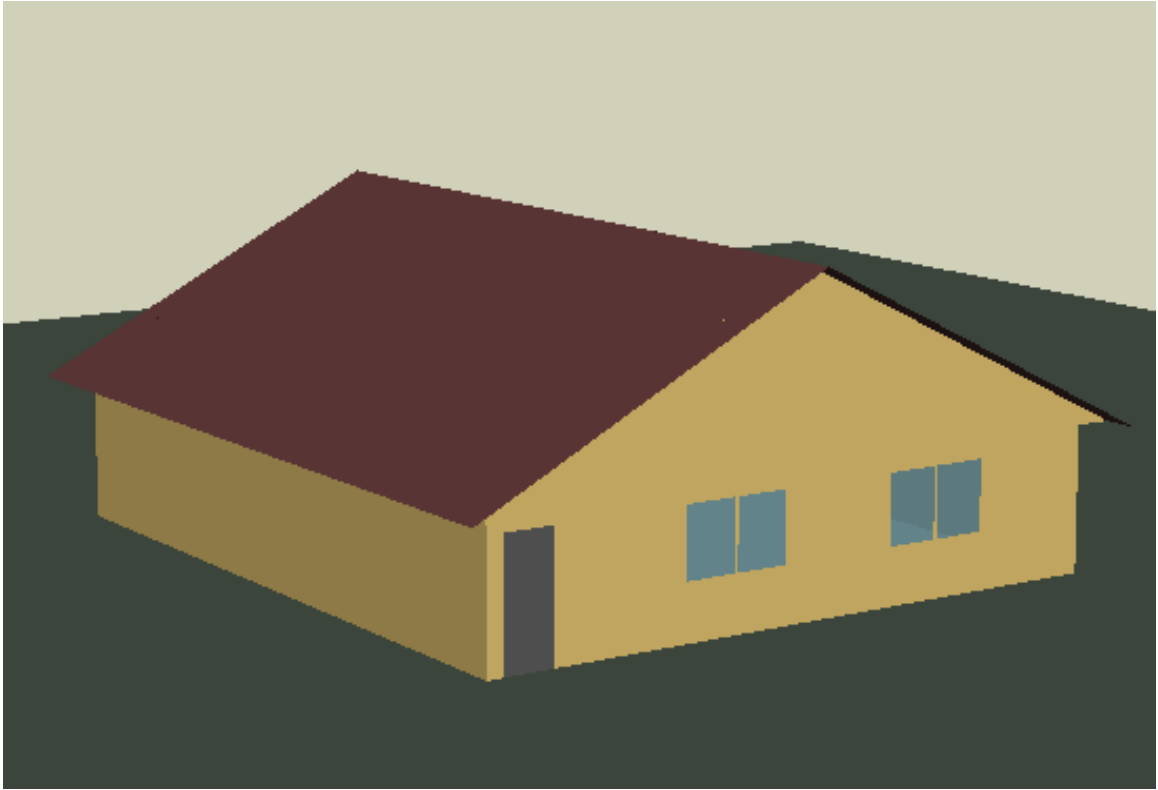


Figure 2.1. EnergyPlus house model developed in BEopt.

Table 2.1. House Parameters

Model attribute	Parameters used
Area	1517 ft^2
No. of floors	1
HVAC system	Electric resistance heating
Window to wall ratio	7%
Glazing layer	2
Glazing material	low-e-glass
Solar heat gain coefficient	0.3
Location and weather file	Chicago, IL

2667.2 kWh, and with a southern orientation was 2620 kWh. However, the energy consumption of the GridLAB-D house model was much higher at 3288 kWh. Most of the difference in energy consumption is due to the different methods EnergyPlus and GridLAB-D use to calculate the ground heat transfer, i.e., heat transfer between the floor of the house and the ground. EnergyPlus uses the ground temperature, whereas in

GridLAB-D the outdoor (air) temperature is used for computing this ground heat transfer. As the outdoor environment temperature is lower than the ground temperature for January, GridLAB-D estimates higher heat loss from the floor and thus higher heating load than EnergyPlus. The ground temperature in general changes at a much slower rate than the outdoor air temperature, leading to large errors in yearly heating/cooling energy uses between the two software simulators, necessitating the use of our HEMS+ co-simulation framework for proper HEMS controller evaluation, which uses the detailed house model of EnergyPlus for estimation of energy consumption and GridLAB-D to model the distribution grid.

2.5 HEMS+ Co-Simulation Framework

The co-simulation framework between EnergyPlus and GridLAB-D, implemented in Python, can be divided into two components: one comprised of the interface to GridLAB-D, and the other of the interface to EnergyPlus, shown in detail in Fig. 2.2. Bus.py, a flexible communication interface, has been used in the co-simulation framework to couple GridLAB-D with the framework [32]. The HEMS+ interface, a communication interface to EnergyPlus, has been developed in this work and, along with Bus.py, forms the overall co-simulation framework. The communication interface between EnergyPlus and the co-simulation framework and the overall co-simulation framework is explained in this section. It is noteworthy that the aggregator, home energy management system, and other controllers can be integrated within the framework. This allows us to validate the control algorithms for residential energy management systems considering the impacts in distribution systems.

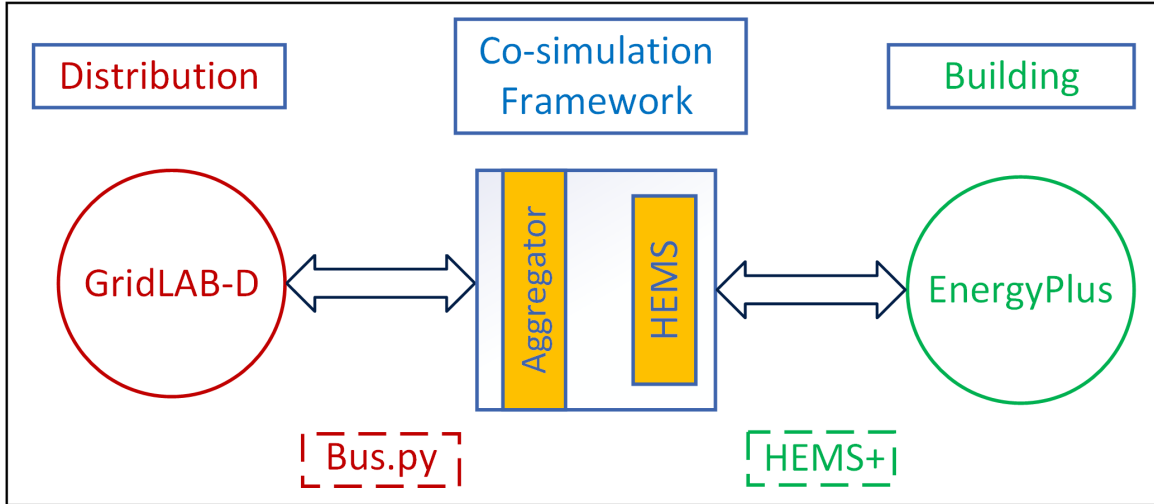


Figure 2.2. Block diagram of co-simulation framework.

Table 2.2. BCVTB Packet Protocol

ver	f	n_d	n_i	n_b	t	v_1	v_2	.	.	.	v_{n_d}
-------	-----	-------	-------	-------	-----	-------	-------	---	---	---	-----------

For the co-simulation of EnergyPlus, a built-in external interface of EnergyPlus enables coupling of EnergyPlus with BCVTB for co-simulation. EnergyPlus exchanges data using an external interface through BSD sockets and a TCP/IP connection. The data packet must follow the BCVTB protocol to be exchanged with EnergyPlus using the external interface. The developed HEMS+ interface implements the BCVTB protocol for data exchange. Each packet of the data contains a sequence of values in the format in Table 2.2. In the data packet, ver represents the version number, f is flag (+1 if simulation reached end time, 0 for normal operation, negative number for error), n_d , n_i , n_b are the number of doubles, integers, and Booleans exchanged, respectively, t represents current simulation time in sec, and $v_1 \dots v_{n_d}$ denotes the variables exchanged. The n_i and n_b are required by EnergyPlus to be set to 0. The number of variables to be exchanged with EnergyPlus is thus represented in n_d . The data is space delimited (0x20) within the packet.

The pseudocode for HEMS+, shown in Fig. 2.3, describes the operation of the

```

1: create_server()
2: run_E+_file()
3: repeat
4:   E+_output = read_from_energyplus()
5:   write_to_energyplus(E+_input)
6: until end of simulation time
7: close_E+_connection()

```

Figure 2.3. Pseudocode for HEMS+ interface.

interface. HEMS+ has five main functions: `create_server`, `run_E+_file`, `read_from_energyplus`, `write_to_energyplus`, and `close_E+_connection`. Each of the functions is described in detail below.

The **`create_server`** function configures HEMS+ as a server for coupling EnergyPlus models. It creates the BSD socket, binds the socket with a socket address and port, and listens for an EnergyPlus connection. The **`run_E+file`** function runs the EnergyPlus building model (.idf) with the specified weather file (typically in .epw format). The `create_server` is configured to accept the EnergyPlus connection and, as EnergyPlus runs, it accepts the EnergyPlus connection to begin the co-simulation. It is important to note that HEMS+ can be configured to accept multiple EnergyPlus models, necessary to co-simulate a large number of houses in the distribution grid as demonstrated in Section 2.6.

After setting up the HEMS+, the simulation loop begins (lines 3–6 of Fig. 2.3). Each iteration of the simulation loop represents one timestep. The **`read_from_energyplus`** function reads and decodes the data packet received from EnergyPlus. This function checks the flag from the packet for an error or end of simulation time during the co-simulation and returns the values of variables received from EnergyPlus. The

write_to_energyplus function encodes the data to be sent to EnergyPlus according to the BCVTB protocol and then sends the encoded data packet to EnergyPlus. The EnergyPlus simulation time is advanced by one timestep. The HEMS+ simulation loop continues until the end of the simulation run time, defined in EnergyPlus model file and co-simulation framework. When the stop time is reached, **close_E+_connection** function closes the connection between EnergyPlus and the co-simulation framework. The variables to be exchanged must be defined in variable.cfg file, as specified by the external interface of EnergyPlus. The readers can refer to [32] for the detailed description of Bus.py interface of HEMS+.

A pseudocode description of the overall co-simulation framework is presented in Fig. 2.4. The functions in italics are from Bus.py and normal fonts are from HEMS+. The co-simulation environment is started by initializing EnergyPlus and GridLAB-D for co-simulation. The **create_server** and **run_E+_file** functions initiate a connection with EnergyPlus. Similarly, **load_bus** reads all the parameters (simulation time information, type of bus, and any other parameters) for Bus.py. The **start_bus** function then starts the GridLAB-D co-simulation. Custom control actions can be taken after line 6 (individual HEMS) and line 7 (aggregator or utility).

After initializing the co-simulation environment, the main loop of the co-simulation (lines 5–9 of Fig. 2.4) is started. Each iteration of this main loop represents one timestep. The single transaction function sends the input to GridLAB-D, increments the GridLAB-D time, and receives the output from GridLAB-D. The **read_from_energyplus** and **write_to_energyplus** functions pass and return variables to EnergyPlus, respectively, and updates the time of EnergyPlus. When the simulation stop time is reached,

```

1: create_server()
2: run_E+_file()
3: Bus = load_bus(input_file)
4: Bus.start_bus()
5: repeat
6:   E+_output = read_from_energyplus()
7:   bus_outputs = Bus.transaction(bus_inputs)
8:   write_to_energyplus(E+_input)
9: until end of simulation time
10: close_E+_connection()
11: Bus.stop_bus()

```

Figure 2.4. Pseudocode for co-simulation framework.

close_E+_connection and **stop_bus** close the EnergyPlus and GridLAB-D connections, respectively.

2.6 Simulation Setup

A case study was conducted to illustrate the usefulness of the co-simulation framework, presented in Fig. 2.5. The residential distribution network from [40] was modeled in GridLAB-D¹. This distribution network has 12 houses and each house was represented by the EnergyPlus house model from Fig. 2.1 with parameters from Table 2.1. For this case study, six houses were instantiated with a northern orientation and six houses with a southern orientation. Each house is assumed to have a HEMS to control its HVAC system, which comprises 27% of the residential energy usage in the U.S. [27], making it a promising candidate for residential DR programs. The HEMS controller (one for each house) calculates and sends the optimal HVAC setpoint temperature to EnergyPlus at each time step. The total power consumed by the house is sent to the distribution network in GridLAB-D to analyze the impact on the distribution system.

¹The EnergyPlus models, GridLAB-D files, and input files are available at <https://github.com/munank/HEMSplus>

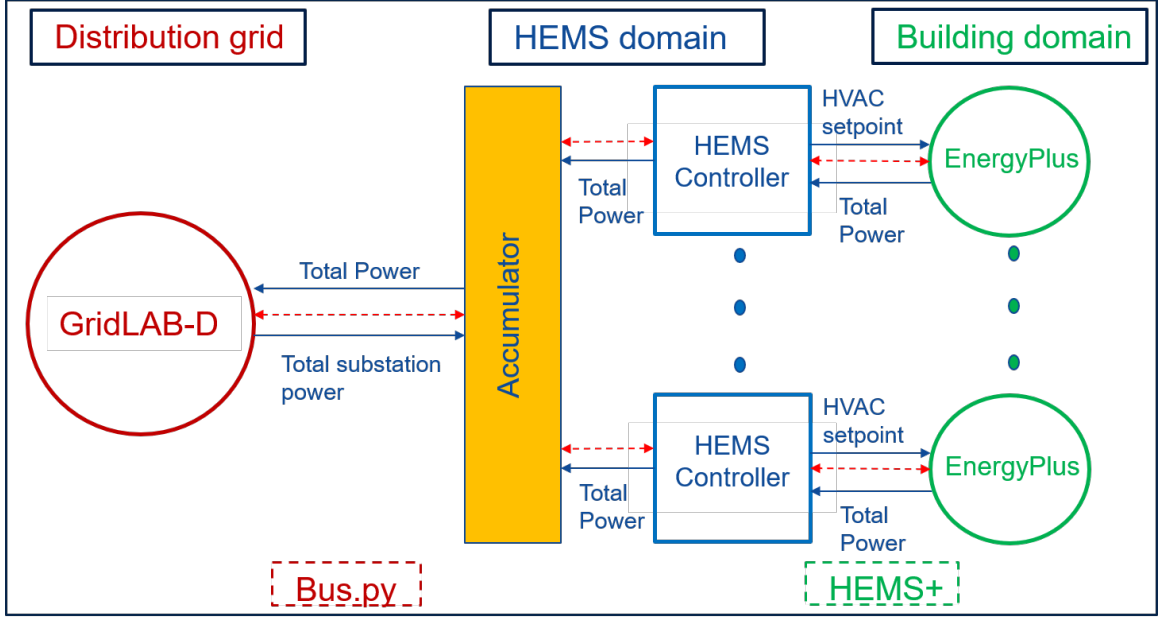


Figure 2.5. Co-simulation case study setup. HEMS controls HVAC system of house and sends the setpoint temperature to EnergyPlus. Accumulator gathers the total house consumption to send to GridLAB-D.

In this work, each HEMS optimizes the HVAC operation to reduce the cost maintaining the room temperature within each consumer's acceptable limits. The linear HVAC model from [41] is used for the optimization. It is important to note that the HVAC model was used only for the optimization, whereas the EnergyPlus model actually calculates the HVAC power in the house. At time t , let θ_t be the room temperature, θ_t^{out} be the outdoor temperature, and p_t be the HVAC power. The next room temperature is then calculated as (2.1).

$$\theta_t = \alpha_1 \cdot \theta_{t-1} + \alpha_2 \cdot p_t + \alpha_3 \cdot \theta_t^{out} \quad (2.1)$$

In the HVAC optimization model, the room temperature at each timestep depends on the previous room temperature, HVAC power, and the outdoor temperature. The values of coefficients α_1 , α_2 , and α_3 were determined by linear regression analysis using the

EnergyPlus house model data for winter months (Nov.-Mar.), and the coefficients were found to be 0.925, 0.61 ($^{\circ}\text{C}/\text{kW}$), and 0.0783, respectively. The model predictive control approach from [41] was used to optimize the thermostat setpoints of the house. The objective function of the optimization is given by (2.2).

$$\min_{p_t \forall t=1, \dots, N_T} C = \sum_{t=1}^{N_T} p_t \cdot \lambda_t \cdot T \quad (2.2)$$

subject to

$$0 \leq p_t \leq p_{max} \quad (2.3)$$

$$\theta_t^{min} \leq \theta_t \leq \theta_t^{max} \quad (2.4)$$

$$\theta_t = \alpha_1 \cdot \theta_{t-1} + \alpha_2 \cdot p_t + \alpha_3 \cdot \theta_t^{out} \quad (2.5)$$

where p_{max} represents maximum power rating of the heating system, θ_t^{max} and θ_t^{min} represent maximum and minimum consumer-defined setpoint temperatures, respectively, λ_t represents the price at time t , and N_T is the number of timesteps.

The simulation is set for the month of Jan. 2017 with a timestep of 15 minutes. Two cases were studied: 1) the base case where the HEMS sends the setpoint temperature to the house model without optimization; and 2) an optimized case where the HEMS sends the optimal setpoint temperature from (2.2) to the house models. For both cases, the base load (other house equipment loads) were generated using queuing theory as described in [14]. The internal heat gain fraction of appliances was assumed to be 0.8 (average heat gain fraction of all appliances) with schedules defined in [39]. Let $\mathcal{N}(\mu, \sigma^2)$ denote a

normal distribution with mean μ and standard deviation σ . For generating resident occupancy schedules, departure and work times were randomly generated from $\mathcal{N}(9.97, 2.2)$ and $\mathcal{N}(7, 1.75)$ [42], respectively, and arrival times were calculated from the departure time and working hours. For the base case, four houses were randomly assigned a constant setpoint temperature throughout day from $[66, 72]^\circ\text{F}$. The setpoint temperature for the remaining houses were motivated by [43], where setpoint temperature varied throughout the day based on occupancy and time of day. For these homes, thermostat setpoint temperature for time $[6, 8]\text{am}$ to departure time, and arrival time to $[10, 12]\text{pm}$ were randomly chosen from $[66, 72]^\circ\text{F}$. The setpoint temperature for the remaining time of day, when the house was empty, was lowered to $[62, 66]^\circ\text{F}$.

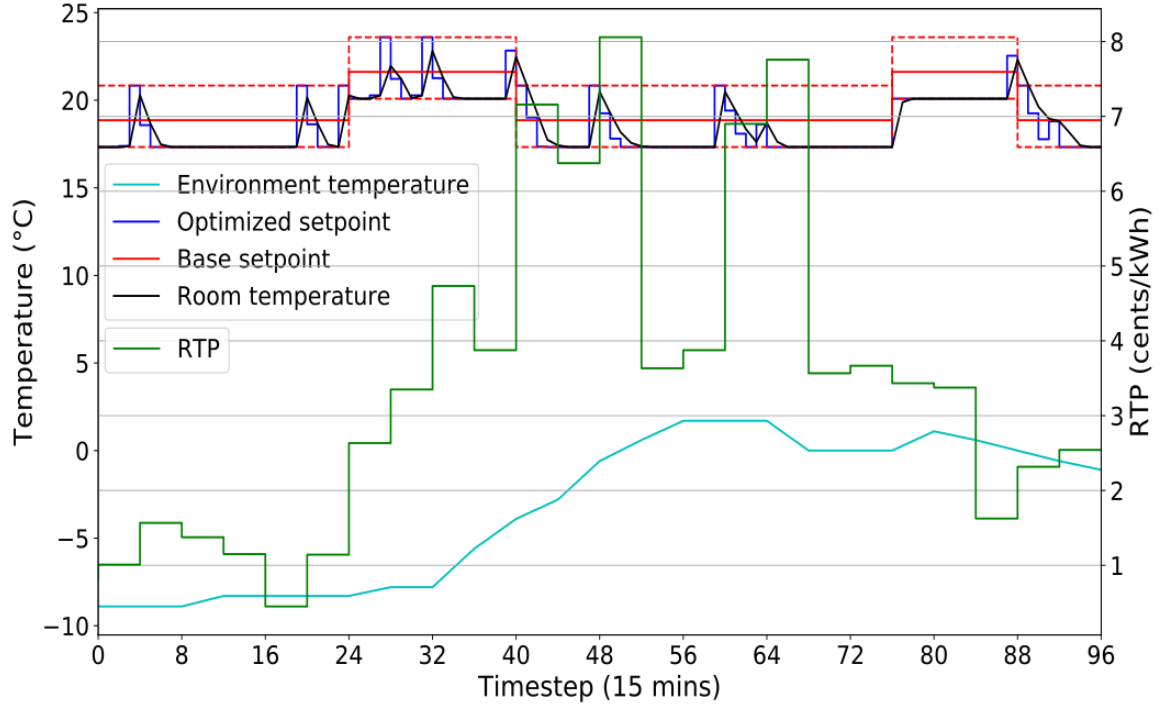
For the optimized case, the HVAC optimization for each house is calculated by each HEMS controller for the entire day (96-timesteps). The HEMS then sends the optimized setpoint at each timestep of the day to the EnergyPlus house models. The HVAC optimization model is formulated in Pyomo [44] and solved using CPLEX. The minimum and maximum allowable temperature for each house were randomly generated from $\mathcal{N}(2, 0.5)$ and $\mathcal{N}(4, 1)$, respectively, inspired by [41], and the real-time price (RTP) in the optimization model was obtained from the hourly RTP published by ComEd, Chicago [45]. It should be noted that these parameters are used only to demonstrate the usefulness of the co-simulation framework, but the framework is general enough to use any parameters.

2.7 Results and Discussion

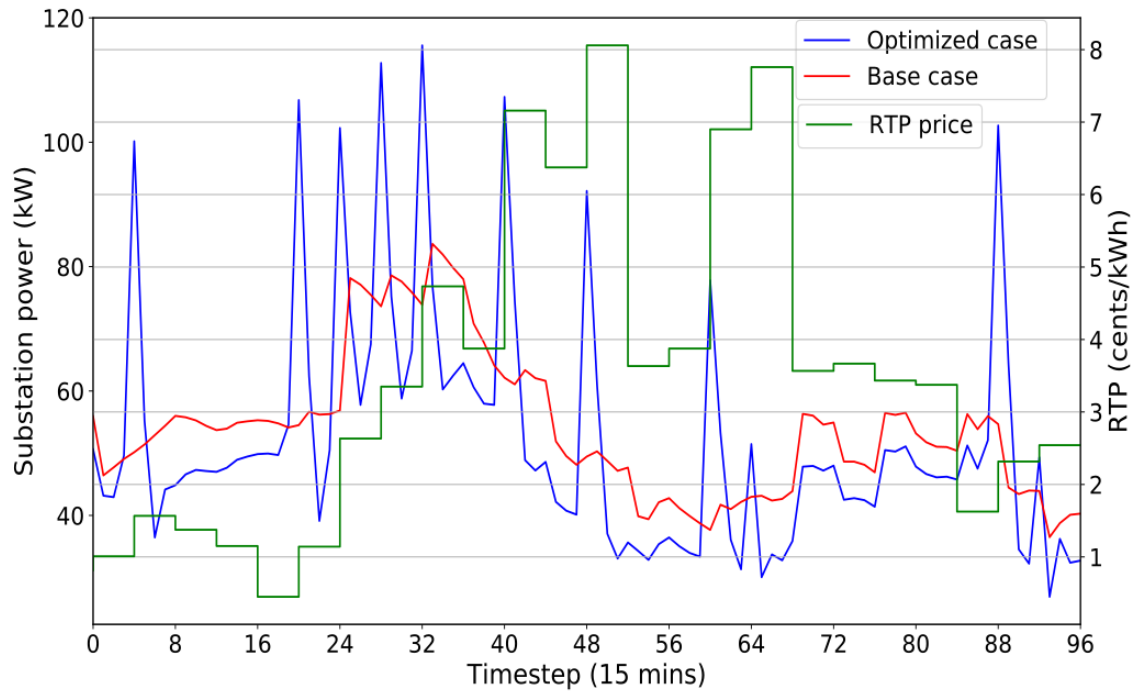
The cases (base and optimized) described in Section 2.6 were simulated for the month of Jan. 2017. The minimum and maximum saving among 12 houses were found to be 4.26% and 7.82% (average saving was 6.45% compared to the base case). The setpoint temperature for both cases for Jan. 9, 2017, along with RTP, is shown in Fig 2.6(a). This particular day is chosen as there were significant fluctuations in the RTP. For the base case, the HEMS disregards RTP and maintains the room temperature according to the setpoint temperature, as explained in Section 2.6. In the optimized case, the room temperature of the house is maintained as per the optimal setpoint temperature, preheating the house before high price periods to minimize the use of HVAC during these times.

Due to fluctuations in RTP, the HEMS of each house greedily alters the thermostat setpoint temperature in accordance with the same RTP signal. The substation power for both cases is shown in Fig 2.6(b). It can be seen that substation power considerably exceeds the distribution transformer power rating in the optimized case when compared to the base case. In the optimized case, the HEMS of each house preheats their house at the same time just prior to the high price period to minimize their cost. Thus, all house HVAC loads coincide, causing large spikes in substation power. Such synchronization of residential loads could potentially cause damage to distribution system equipment, motivating the need for coordination and/or non-greedy methods between HEMS of various houses, and co-simulation with the distribution grid.

The substation power for both cases for Jan. 21 is presented in Fig 2.7. On this day, the fluctuations in RTP were not significant and only occasional preheating of houses was



(a)



(b)

Figure 2.6. (a) Setpoint temperature for House 1 on Jan. 9, 2017. The room temperature (solid black curve) follows optimal setpoint temperature (solid blue line) in the optimized case. The maximum and minimum allowable setpoint temperature is represented by the solid red line. (b) The comparison between substation power for base (solid red curve) and optimized case (solid blue curve). The RTP is represented by the solid green curve.

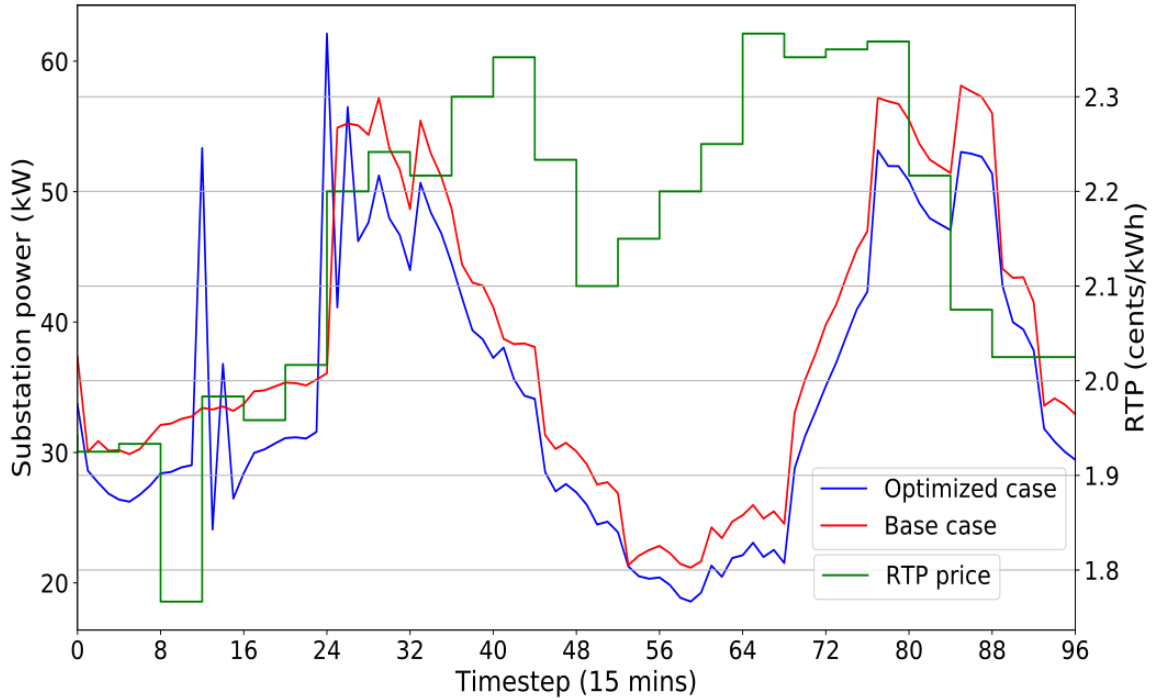


Figure 2.7. Comparison between substation power for base (solid red curve) and optimized (solid blue curve) cases for Jan. 21.

observed. This reduced the number of spikes in substation power in the optimized case compared to substation power in Jan. 9.

2.8 Conclusion

This chapter presents a novel co-simulation framework for coupling EnergyPlus and GridLAB-D. Controllers, such as HEMS and aggregators, can be easily incorporated into the co-simulation framework allowing design, testing, and validation of control algorithms for residential energy management while considering distribution impacts. The framework, implemented in Python, uses the pre-existing Bus.py for co-simulating GridLAB-D with the framework, and developed the HEMS+ interface to connect EnergyPlus with the framework. The case study demonstrates the feasibility and usefulness of the co-simulation framework. Though we have presented a single case study

demonstrating residential energy management, the generalized framework can be extended for any energy management algorithm and for commercial building optimization. The case study showed that greedy HEMS optimization based on the same pricing signals causes system peaks more severe than normal operating conditions. This showcases the need for the co-simulation framework presented in this work that models in detail many homes and verifies grid impacts, allowing for future Smart City simulations.

CHAPTER 3 SMART HOME ENERGY MANAGEMENT SYSTEM IN THE CO-SIMULATION FRAMEWORK

3.1 Background

Financial incentives play an important role in encouraging residential consumer participation in DR programs. Consumers are generally motivated to participate in such DR programs by offering an incentive (incentive-based DR), or by introducing the time-varying tariff for electricity consumption (price-based DR) such as TOU, RTP, CPP etc as explained in Chapter 1. Price-based DR intends to encourage the consumers to shift the energy consumption away from high price period or to curtail the energy consumption during the high price periods for financial benefits. With the time-varying tariff, manually changing the electricity consumption for the residential consumers is cumbersome which ultimately discourages the residential consumers to participate in such DR programs. HEMS plays a key role by automatically altering the energy consumption pattern of the consumers according to the time-varying tariff. HEMS can also consider consumer comfort during scheduling of the appliances.

A preliminary HEMS considering the scheduling of HVAC setpoint is presented in Chapter 2 for the demonstration of the co-simulation framework. In this chapter, a detailed formulation of HEMS considering the combined scheduling of HVAC as well as appliances is presented. The HVAC model of Chapter 2 is further improved to incorporate the internal heat gain of the appliances. During the scheduling of the HVAC and appliances, HEMS also considers the residential consumers' comfort.

3.2 Related works

In recent years, several home energy management system algorithms have been developed for managing residential end-uses. The authors in [9] proposed the convex optimization to minimize the total cost and user dissatisfaction. A mixed integer linear programming (MILP) optimization is proposed in [11], smart scheduler in [10], and two horizon in [13] for scheduling the appliances of the house including the photo-voltaic (PV). In [12], MILP and heuristic algorithm determines the consumer load profile based on the price signals received from the aggregator. In [46], stochastic and robust optimization approaches, formulated as MILP problem, schedule the thermal and non-thermal appliances based on the price signal. However, combined scheduling of thermal and non-thermal appliances considering the effect of appliance heat gain on HVAC operation has not been considered in [9]–[13], [46]. Two partially observable Markov decision process (POMDP) approaches are proposed in [14] for scheduling appliances with the objective of minimizing the total electricity cost in RTP tariff. But, only non-thermal appliances are considered in [14]. Also, detailed house model for evaluating the performance of the proposed HEMS has not been considered in the above literature.

The combined scheduling of the home appliances as well as electric vehicles (EVs) to minimize the cost, as well as consumer discomfort has been investigated in [47]. Similarly, in [48], dynamic programming is used to manage the controllable loads as well as EVs. A bottom-up approach is used for generating highly resolved energy consumption models. The detailed building thermal model is not considered in [47], [48] where the main focus of authors is combined scheduling of home appliances and EVs. A

chance-constrained optimization model in [49], solved using improved particle swarm optimization and two-point estimate, a quadratic stochastic optimization model in [50], and real-time optimization-based model in [51] are proposed to account the uncertainties in the HEMS.

Similarly, in [20], HVAC control strategy considering the house model in EnergyPlus is developed. In this work, a linear change in setpoint of the thermostat based on price and preference is proposed. Comparison of ON/OFF control, proportional–integral–derivative (PID) control, and model predictive control (MPC) for controlling AC are shown in [22]. The aggregated effect of MPC on a large number of residential consumer's AC is presented in [21]. A reduced RC model was developed for representing the building thermal model and compared with EnergyPlus model. Though a detailed thermal model is considered in [20]–[22], authors considered only thermal appliance without considering the non-thermal appliances for scheduling.

Different meta-heuristic and heuristic methods have also been proposed for HEMS. In [15], genetic algorithm (GA) is used to minimize the cost as well as peak to average ratio (PAR) of residential energy consumption. A combination of RTP and inclining block rate is proposed. In [16], genetic binary particle swarm optimization is proposed to minimize cost and PAR and compared with other heuristics methods such as GA, wind-driven optimization (WDO). A binary backtracking search algorithm is proposed in [17], binary particle swarm optimization in [18], wind driven optimization in [19] for scheduling the residential appliances.

3.3 Proposed work

In summary, the combined scheduling of the HVAC and the other appliances considering the heat gain of the appliances has not been considered in the previous studies. The internal heat gain of the appliances affects the operation of HVAC in summer as well as winter months. Thus, while considering optimal scheduling of appliances and HVAC setpoint temperature, a combined scheduling approach of appliances, as well as HVAC setpoint incorporating the heat gain of scheduled appliances needs to be considered. The proposed smart HEMS in this work considers integrated scheduling of the HVAC and appliances to reduce the overall electricity bill of the consumer. This work also proposes an HVAC model to consider the heat gain of the appliances. The residential consumer preferences are considered during the scheduling process for maintaining the resident's comfort. The smart HEMS also considers detail house model in EnergyPlus. The detailed model allows evaluating the effectiveness of the proposed HEMS. The HEMS+ co-simulation framework explained in Chapter 2 is used for coupling the proposed HEMS and EnergyPlus house model.

3.4 Model Description

The residential appliances consist of thermostatic appliances such as HVAC and water heater and non-thermostatic appliances such as plug loads. The detail description of the residential appliance models such as HVAC model and appliance model is explained in this section. Similarly, the description of the house model considered in the work is provided in this section.

3.4.1 House Model

A single family detached house model, presented in Chapter 2.4, is used for this study. A 1-stage central air conditioner (AC) with seasonal energy efficiency ratio (SEER) of 13 is considered for the cooling system whereas an electric baseboard heater is considered for the heating system. SEER represents ratio of total heat removed from the conditioned space to total electrical energy consumed. The benchmark for SEER rating for AC is 13 as described in [52]. A constant air change per hour (ACH) of 0.1 is assumed for the simplification of the house model. ACH represents the air leakage into a building and is the ratio of air volume change rate to volume of the space.

3.4.2 HVAC Model

The linear model for the calculation of the indoor temperature of the house from [41] is given by (3.1). According to this model, the indoor temperature of the house (θ_t) depends on the previous room temperature (θ_{t-1}), HVAC power ($p_{hvac,t}$), and outdoor temperature (θ_t^{out}). The α_1 , α_2 , and α_3 are the coefficients of the previous room temperature, HVAC power, and outdoor temperature respectively which are determined by the linear regression method. This HVAC model does not account for the internal heat gain of the appliances.

$$\theta_t = \alpha_1 \cdot \theta_{t-1} + \alpha_2 \cdot p_{hvac,t} + \alpha_3 \cdot \theta_t^{out} \quad (3.1)$$

The linear HVAC model from [41] is modified so as to include the internal heat gain of the appliances. The inclusion of the appliance heat gain improves the accuracy of the HVAC model and thereby HVAC model can more precisely predict the house temperature.

Such inclusion is also important while considering the combined scheduling of HVAC and appliances in HEMS. The modified HVAC model given by (3.2). The α_4 is the coefficient given to the internal heat gain from the appliances. Here, p_a represents the power consumed by each appliance 'a' and G_a represents the internal heat gain of each appliances.

$$\theta_t = \alpha_1 \cdot \theta_{t-1} + \alpha_2 \cdot p_{hvac,t} + \alpha_3 \cdot \theta_t^{out} + \alpha_4 \cdot \sum_{a=1}^n p_a \cdot \delta_{a,t} \cdot G_a \quad (3.2)$$

For the comparison of the two models for the winter month, we simulated the house model, described in the previous subsection, in 1-minute timestep for November - March. The house model has the appliance schedules and internal heat gain as described in building America house simulation protocol [52]. The temperature setpoint of the house in EnergyPlus was perturbed within 21.67°C (71°F) and 22.23°C (72°F). The variation in temperature setpoint is necessary for generating deviation in room temperature and previous room temperature for training the coefficients of the HVAC model. We then used linear regression to calculate the each coefficients of the both models represented in (3.1) and (3.2).

The coefficients α_1 , α_2 , and α_3 for HVAC model in (3.1) were calculated as 0.9949, 0.0542 ($^\circ\text{C}/\text{kW}$), and 4.185×10^{-3} respectively. Similarly, for the HVAC model in (3.2), the coefficients α_1 , α_2 , α_3 , and α_4 were estimated as 0.9936, 0.0547 ($^\circ\text{C}/\text{kW}$), 4.278×10^{-3} , and 0.0318 ($^\circ\text{C}/\text{kW}$) respectively. It is noteworthy that as the timestep of the simulation is 1 min, the indoor temperature mainly depends on the previous room temperature on the both model. The HVAC power of EnergyPlus, estimated HVAC power

of HVAC models ((3.1) and (3.2)) for maintaining a temperature setpoint of 21.67°C (71°F) were computed for month of January. On comparing the HVAC power of HVAC model without heat gain (3.1) with EnergyPlus, the root mean square error (RMSE) for the month was found to be 0.345 kW whereas the RMSE was 0.22 kW in case of HVAC model with heat gain (3.2). The comparison of predicted HVAC power of both HVAC model with EnergyPlus for a day (January 25) is shown in Fig. 3.1.

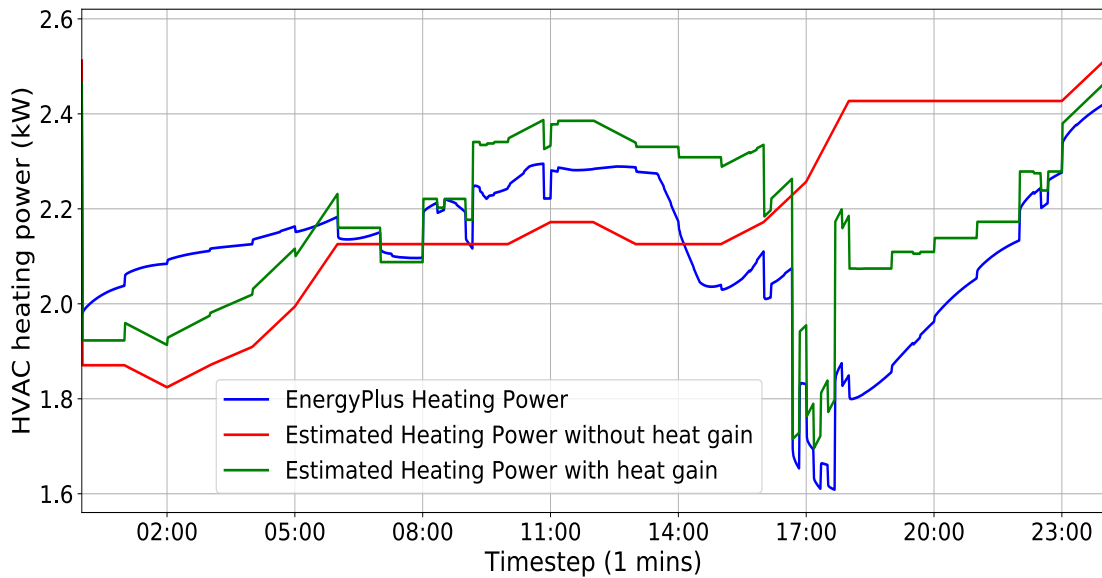


Figure 3.1. Comparison of power consumption of HVAC models with EnergyPlus. The HVAC model with heat gain (solid green curve) estimate the energy required by HVAC to maintain setpoint temperature accurately compared to HVAC model without heat gain (solid red curve)

The inclusion of the appliance heat gain improves the accuracy of the model as can be seen in Fig. 3.1. This would be more critical in the HEMS where the appliances are shifted thus shifting the heat gain from the appliances. This necessitates the combined optimization of the appliance and HVAC considering heat gain of appliances.

3.4.3 Appliance Model

Appliance load for a house is generated using $M_t/G/\infty$ queue model from [14]. This model generates unique loads for each house such that the aggregate load of all houses matches the distribution system load profile. The hourly load data of the distribution system is used as input to the queue model. An expected aggregated home load, $l(t)$, is scaled down from the distribution system load by (3.3). At time t , $C_l(t)$ represents the total distribution load, and b_{min} and b_{max} represents scaling factors.

$$l(t) = b_{min} + \frac{C_l(t) - \min(C_l)}{\max(C_l) - \min(C_l)} \cdot (b_{max} - b_{min}) \quad (3.3)$$

The model then generates the appliance loads assuming constant power generic appliance model. For each of the appliance a , the queue model generates the arrival time of the appliances t_a^{arr} , duration of the appliances t_a^{dur} , as well as power rating of the appliances p_a^{rated} . Readers can refer to [14] for a more detailed explanation of the queue model.

3.5 Description of HEMS framework

The system block diagram of the proposed HEMS is shown in Fig. 3.2. The detailed model of the residential house is modeled in EnergyPlus. HEMS optimization calculates the optimized HVAC setpoint and the appliances schedules based on the price and consumer preferences. HEMS optimization utilizes the linear HVAC model and appliances explained in Section 3.4 in the optimization. Consumer preferences, price, and weather data are provided to HEMS optimization. HEMS+ represents a co-simulation framework between HEMS and EnergyPlus. HEMS+ allows sending the optimal HVAC

setpoint as well as appliance schedule to the EnergyPlus house model for calculating the energy consumption and also send the total energy consumption to the HEMS controller.

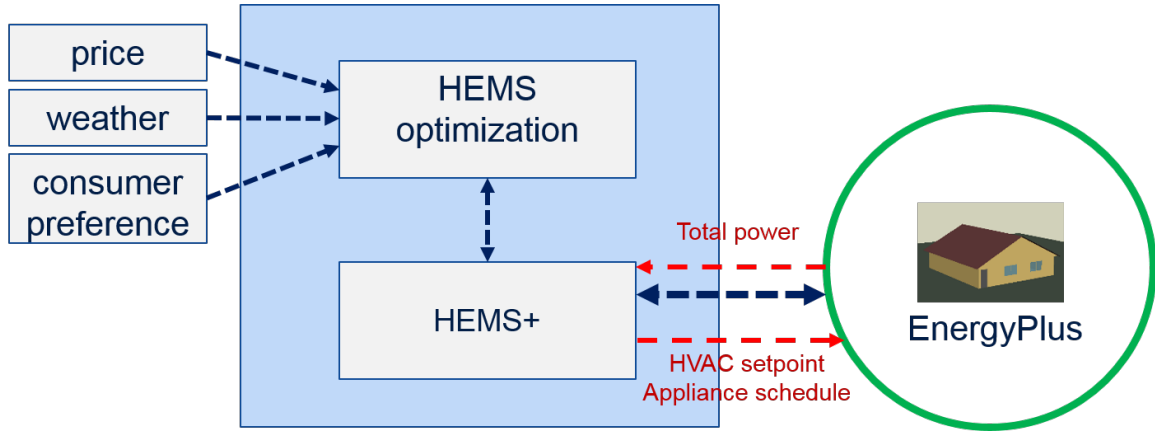


Figure 3.2. A system block diagram of the proposed HEMS. HEMS optimization calculates the optimized HVAC setpoint and appliance schedule and sends the optimal schedule to building model in EnergyPlus using HEMS+. The detailed EnergyPlus building model calculates the total power consumption of the house.

3.5.1 Co-simulation Framework

The developed co-simulation interface HEMS+ explained in Chapter 2 is used as the co-simulation interface between HEMS and EnergyPlus.

3.5.2 HEMS optimization

The HEMS optimization determines the optimal setpoint temperature of the house as well as the scheduling of the appliances. The objective of the proposed HEMS optimization is to minimize the electricity bill as shown in (3.4). Here, λ_t represents the time-varying tariff rate such as RTP (\$/kWh), $p_{hvac,t}$ represents HVAC power (kW), p_a represents rated appliance power (kW), and $\delta_{a,t}$ is the on/off status of appliance a at time t . Here n is the total number of appliances and N_T represents the optimization horizon.

$$\min_{p_{hvac,t}, \delta_{a,t}, \theta_t} C = \sum_{t=1}^{N_T} \lambda_t \cdot T \cdot (p_{hvac,t} + \sum_{a=1}^n (p_a \cdot \delta_{a,t})) \quad (3.4)$$

subject to power limit (3.5), HVAC constraints (3.6) - (3.8), and appliance constraints (3.9) - (3.13).

Power limit constraint: The power limit constraint (3.5) assures that the total power consumption of the house at any particular time t is within the total power limit of the house. This power limit of the house is dictated by the limit of the main circuit breaker of the house.

$$p_{hvac,t} + \sum_{a=1}^n (p_a \cdot \delta_{a,t}) \leq P_{limit} \quad (3.5)$$

HVAC constraints: Equation (3.6) governs the total power consumption to be between 0 and maximum power rating of the HVAC ($p_{hvac,max}$). Constraint (3.7) regulates the temperature of the house between the minimum and maximum allowable temperature set by the consumer. It is noteworthy that the minimum and maximum temperature (θ_t^{min} and θ_t^{max} respectively) represents the preference of consumer in terms of comfort and depends on consumer preference. Equation (3.8) represents the HVAC model for model predictive control (MPC) which predicts the temperature of the house for the optimization.

$$0 \leq p_{hvac,t} \leq p_{hvac,max} \quad (3.6)$$

$$\theta_t^{min} \leq \theta_t \leq \theta_t^{max} \quad (3.7)$$

$$\theta_t = \alpha_1 \cdot \theta_{t-1} + \alpha_2 \cdot p_{hvac,t} + \alpha_3 \cdot \theta_t^{out} + \alpha_4 \cdot \sum_{a=1}^n p_a \cdot \delta_{a,t} \cdot G_a \quad (3.8)$$

Appliance constraints: Equations (3.9) - (3.13) are the constraints that governs the operation of the appliances of the house. Constraint (3.9) guarantees that the total energy consumption of the remains same and ensures that each appliance operates for the fixed operating duration of the appliance. Constraint (3.10) indicates that start time of the appliance. Constraint (3.11) is the un-interruption constraint ensures that each appliance is only started once and not interrupted during their operation. Constraint (3.12) and (3.13) shrinks the search space for the optimization by eliminating the possibility of start/working of the appliance at time beyond consumer preference. The consumers specify the allowable start and end time of the appliance per their convenience.

$$\sum_{t=ts}^{te} \delta_{a,t} = duration_a \quad \forall a \in [1, n] \quad (3.9)$$

$$\delta_{a,t+1} - \delta_{a,t} - z_{a,t} \leq 0 \quad \forall a \in [1, n] \quad (3.10)$$

$$\sum_{t=1}^{N_T} z_{a,t} = 1 \quad (3.11)$$

$$\delta_{a,t} == 0 \quad \forall a \in [1, n], \quad t \notin [ts, te] \quad (3.12)$$

$$z_{a,t} == 0 \quad \forall a \in [1, n], \quad t \notin [ts, te] \quad (3.13)$$

3.5.3 Model predictive control

The proposed HEMS scheduling problem is formulated on the model predictive control (MPC) framework. MPC is any control method that utilizes the concept of prediction and obtains the control signal by minimizing a certain objective function while satisfying a set of constraints [53]. MPC incorporates the model (such as HVAC and appliance model for HEMS) for deriving the optimal control actions. In MPC, system information is updated in each timestep of MPC, resulting in different optimization problem at each MPC timestep. Thus, the optimization problem is solved at each timestep of MPC and the control actions at given timestep are only implemented. The updated system information provides an initial condition for prediction and thereby decreases the error in the prediction. In the proposed HEMS system, the updated information of the system includes the updated information of the indoor temperature of the house and current appliance status.

The difference in proposed HEMS MPC formulation is the prediction horizon of the MPC. Generally, in MPC, the prediction horizon of the MPC is fixed i.e. that the controller predicts the control action for certain 'N' timestep ahead at each current timestep. The utilities such as ComEd provides the DAP for the next day at approximately 5 PM and RTP (the price consumer is billed) is calculated on an basis [45]. In order to utilize all the available price data, the proposed HEMS have fixed time for prediction horizon and decreases the prediction horizon as time moves forward. Explaining with an example, let us consider the HEMS is calculating control action at 9 A.M as shown in Fig. 3.3. The prediction horizon of the HEMS, in this case, is 12 A.M midnight of the

same day. But, as HEMS receives updated DAP for the next day at 5 P.M, the prediction horizon for HEMS at 5 P.M is till 12 A.M the next day. As HEMS move forward in time, the prediction horizon timestep decreases till HEMS receives DAP update at 5 P.M.

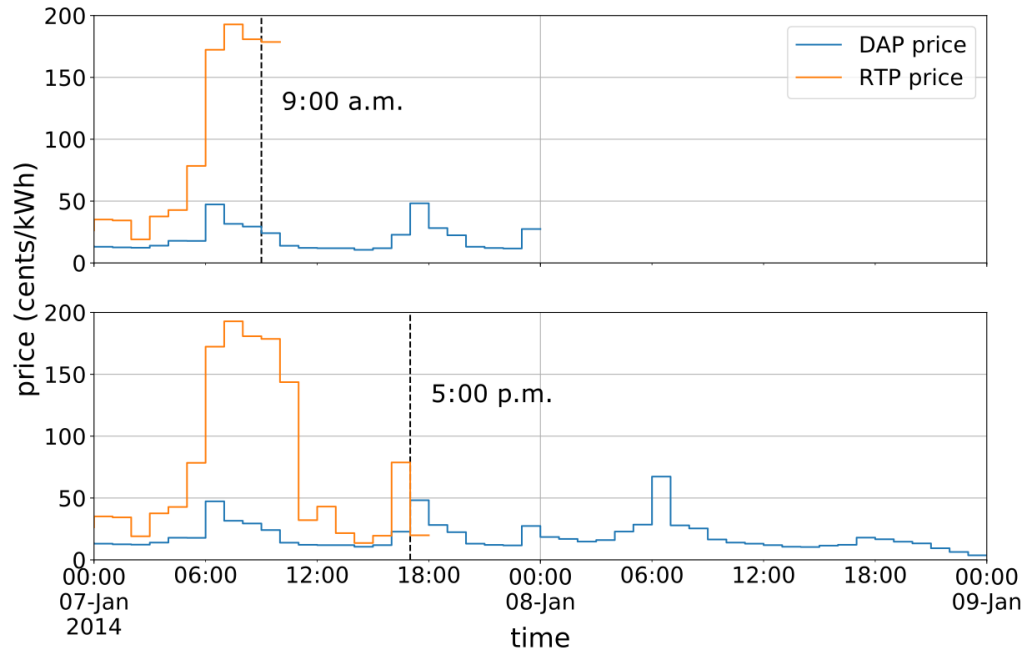


Figure 3.3. An example of ComEd residential time-varying tariff [45].

3.5.4 Overall algorithm

The overall algorithm of the HEMS is explained in Algorithm 1. In the initial setup, the HEMS receives the consumers' preferences (HVAC setpoint temperature and the appliance preferred schedule and acceptable deviations from their predefined schedule for the day) from the residential consumer. HEMS also receives weather data as well as the price information for the day. It is noteworthy that the price signal for the entire prediction horizon and the weather information updates each day and the HEMS schedule the HVAC setpoint and the appliance schedule considering price and weather information.

As explained in the previous subsection, in each timestep of MPC, the HEMS perform optimization based on the receding-horizon MPC approach. Though the HEMS calculates the optimal schedule for the overall horizon, only the current timestep optimal HVAC setpoint and appliance schedule is sent to EnergyPlus via HEMS+. The EnergyPlus then calculates the energy consumption of the house based on updated HEMS control signals. The EnergyPlus then sends the total power consumption of the HEMS to the HEMS via. HEMS+. Then, time is advanced by ΔT in both HEMS and EnergyPlus. We have considered that the DAP price information is updated at 5 PM as in ComEd. The same process is repeated until we reach the end time of the simulation.

Algorithm 1: Overall HEMS algorithm

- 1: Receive the consumer preferences, weather data, and price information
 - 2: **while** $t \leq T_{end}$ **do**
 - 3: Update price and weather data. Update consumer preference if consumer updated their preferences.
 - 4: Perform HEMS optimization with objective of minimizing total cost (3.4) subjected to the constraints (3.5)- (3.13)
 - 5: Send the optimal HVAC setpoint and appliance schedules via HEMS+
 - 6: Calculate the total power consumption of house using detailed house model in EnergyPlus
 - 7: Receive total power consumption of house from EnergyPlus model via HEMS+
 - 8: Advance time t by ΔT in HEMS optimization as well as EnergyPlus
 - 9: **end while**
-

3.6 Simulation Setup

For evaluation of the proposed smart HEMS, five different test cases were considered. The five test cases compare the different scenarios with HEMS (with or without perfect price information and combined scheduling of HVAC and appliances) and a base case without HEMS. Such comparison of combined scheduling of HVAC and appliances with independent optimization of HVAC and appliances under different price

information quantifies benefits of the co-optimization of HVAC and appliances.

1. Base case: In this case, the HVAC operates with their predefined setpoint and the appliances operates in the assigned start time provided by the consumer. It is assumed that the house does not have the capability of HEMS and thereby, does not schedule HVAC setpoint as well as appliance according to time-varying rate.
2. Case-I: In this case, we assume HEMS have perfect price knowledge of the time-varying RTP of the prediction horizon beforehand. Since HEMS possess RTP information, it can optimize to generate optimal HVAC setpoint and appliance schedule. The HVAC model, in this case, is defined in (3.2) and combined scheduling of HVAC and appliances are considered. In fact, this case provides the upper bound in saving due to HEMS for the consumers.
3. Case-II: The HEMS in this case also have perfect price knowledge as in Case-I. But the HVAC model in the HEMS optimization, as defined in (3.1), does not consider heat gain of appliances.
4. Case-III: In this case, we assume that the HEMS have access to the RTP of the current hour only and do not have the complete RTP information of the prediction horizon (as in Case-I). Since utilities provide the DAP a day before, HEMS utilizes the DAP for the optimization for the rest of the hours whereas uses RTP for the current hour. It is noteworthy that the residential consumers are billed with the RTP only. The integrated appliance and HVAC scheduling is considered as the HVAC model for HEMS optimization, in this case, is (3.2). It is the realistic scenario for HEMS as it utilizes available price information for the optimization.

5. Case-IV: This case is the same as Case-III except for the HVAC model in the optimization is (3.1).

For all the cases, the house model explained in Section 3.4 was modeled in the EnergyPlus. We have considered the location of the house as Chicago, IL and used the typical meteorological year (TMY3) weather file for Chicago as weather file for the EnergyPlus house model. As for the time-varying tariff rate, we have used the RTP and DAP provided by ComEd, a utility company in Chicago, as input for the HEMS [45]. For Case - III and Case- IV, DAP information for the next day is updated at 5 PM each day. Similarly, we have considered actual RTP information of the next day is updated at 5 PM for Case - I and Case - II for a fair comparison. The total power limit of the house was considered as 15 kW [54].

For the simulation purpose, the PJM load was used in the queue model to generate the appliance load for the house. The scaling factors b_{min} and b_{max} were set to 100 W and 5000 W respectively. Each appliance is randomly assumed to have the maximum flexibility of 1h, 2h, 4h, and 8h from the scheduled time [14]. The house model is assumed to have setpoint temperature according to [43] for the Base case. For case (I-IV), it is assumed that maximum allowable temperature to be 2 °C above base case setpoint and minimum allowable temperature to be 1 °C below the base case setpoint. The flexibility of appliances and HVAC setpoint temperature depends on each consumer but the HEMS framework is flexible to incorporate individual consumer preference.

We have considered both summer as well as winter months for evaluation of the performance of the proposed HEMS. The statistical analysis of the RTP of ComEd for

Table 3.1. Price data for various months

Month	Max. price (cents/kWh)	Min. price (cents/kWh)	Mean price (cents/kWh)	S.D (cents/kWh)
Jun 2008	48.70	-21.1	5.95	6.18
Jan 2014	192.81	-4.72	6.75	15.98
Jan 2017	11.04	0.45	2.83	1.07

different months is presented in Table 3.1. The HEMS optimization is performed every hour and the timestep in each optimization is 1 min. Thus, the control signals (HVAC setpoint and appliance schedule) are generated for every minute.

3.7 Results and Discussion

3.7.1 Winter Months

For training the coefficients of the HVAC model for winter months, the EnergyPlus model described in Section 3.4 was simulated for months of November - March. The temperature setpoint of the building model was set between $[21.67^{\circ}\text{C}, 22.23^{\circ}\text{C}]$ with a timestep of 1 min. The appliance schedule and its heat gain were used as described in building America house simulation protocol [52]. We have used linear regression model and least square estimation technique for determining the coefficients of both HVAC model defined in equations (3.1) and (3.2). The coefficients of the winter HVAC models are presented in Table 3.2. The large value of α_1 compared to other coefficients indicates that the room temperature is mainly dependent on previous room temperature. This is due to the timestep of building simulation of 1 min.

The total savings for different cases for several months is presented in Fig. 3.4. For the month of January 2014, the total savings for Case-I is 23.3% which represents the upper bound for HEMS savings. Comparing total savings of Case-I and Case-III, we can

Table 3.2. HVAC model coefficients

Months	HVAC model	α_1	α_2 (°C/ kW)	α_3	α_4 (°C/ kW)
winter	(1)	0.9949	0.0542	0.004185	-
winter	(2)	0.9936	0.0547	4.28×10^{-3}	0.0318
summer	(1)	0.9956	-0.153	0.00573	-
summer	(2)	0.995	-0.0167	4.81×10^{-3}	0.00441

observe that HEMS can result in significant saving with perfect price information. This discrepancy between the total saving of Case-I and Case-III is due to high variation in the price in January 2014, indicated by the standard deviation of RTP price in Table 3.1. The total savings for January 2014 is higher for cases with improved HVAC model (3.2) compared to cases with HVAC model represented by (3.1). It indicates that HEMS performance and saving can be improved with the co-optimization of HVAC and appliances.

For the month of January 2017, the maximum HEMS saving in Case-I with perfect price information is 9.7%. This is because of less variation in the RTP prices as can be seen in Table 3.1. The HEMS saving in Case-III is equal to the total saving in Case-II. This means that for this month, co-optimization of HVAC and appliances with imperfect price information resulted in the same saving as optimization with perfect price information and independent optimization of HVAC and appliances.

The total house power for the different cases can be seen in the Fig. 3.5 represented by a solid red line. Explaining the working of HEMS, the HEMS reduces the energy consumption during the high price period and schedules the load in the low price period to reduce the electricity bill of the consumer. HEMS accounts for the consumer flexibility during the scheduling of HVAC and appliances. In Case-I and Case-II with the perfect

price knowledge, HEMS is capable to perfectly schedule the load to minimize the total cost. In contrast, in Case-III and Case-IV without the perfect price information, HEMS may fail to identify the lower price regions of the day and thus cannot obtain the theoretically possible minimum price bound. For instance, we can see that at 3 - 4 AM in Fig. 3.5, HEMS in Case-I identifies the current RTP as low price and schedules the available load in the particular hour. But in Case-III and Case-IV, with only DAP information for rest of the prediction horizon, HEMS does not identify the hour 3 - 4 AM as low price and therefore does not shift available load in this hour. Thus, for the months such as January 2014, there is significant saving potential with the use of the improved price forecast techniques instead of using DAP prices as shown by the total savings of Case-I and Case-III. Employing a more accurate price forecast is out of the scope of this work.

It is interesting to understand the scheduling of components of the house (appliance and HVAC) by the HEMS. The total electricity cost comprising of HVAC cost and appliance cost for winter months are presented in Table 3.3. Comparing the appliance cost for different cases, there is significant saving from appliance shifting for all cases I-IV

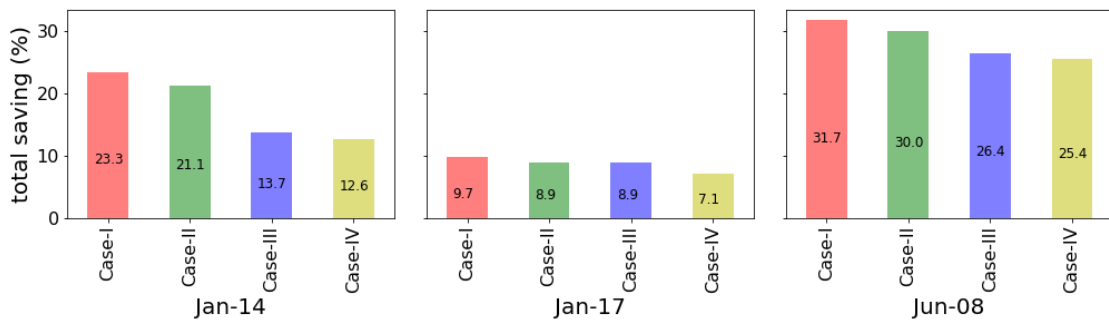


Figure 3.4. Comparison of total savings of the different months for each cases.

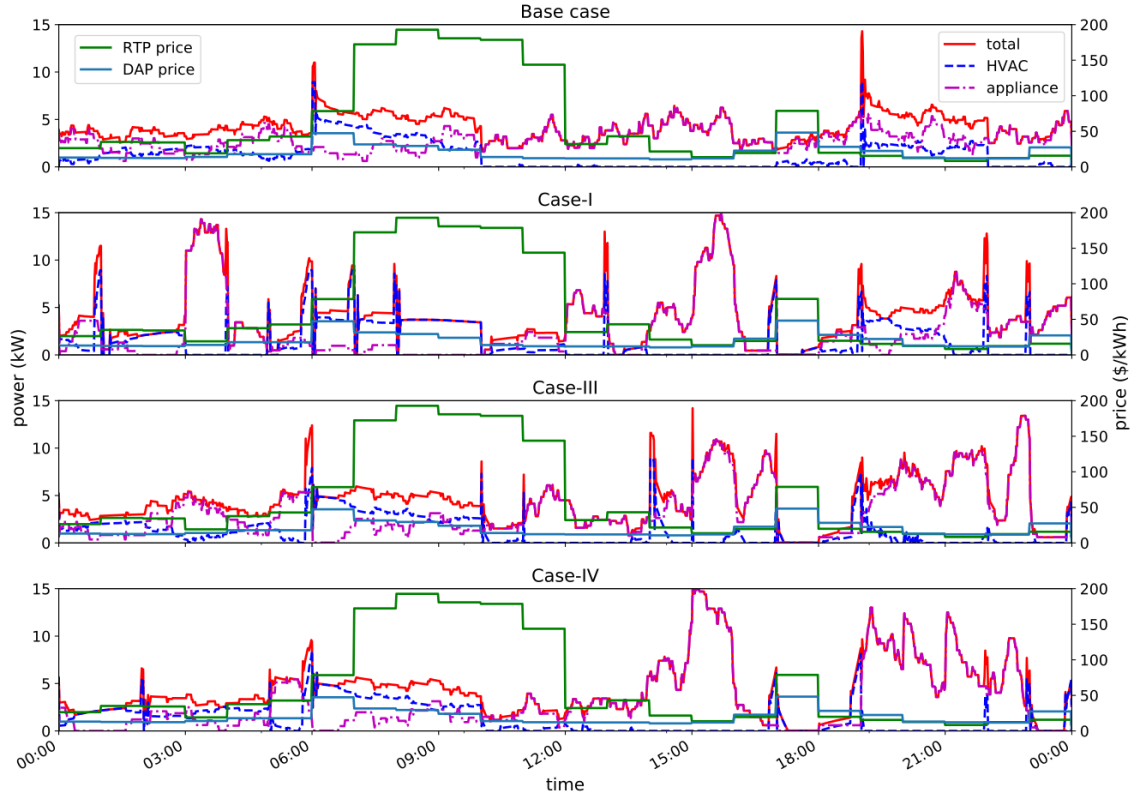


Figure 3.5. HVAC, appliance, and total house power for each case on January 7, 2014. Each subplot represents the total house power for different cases for the particular day. The solid green curve represents RTP price and solid light blue curve represents DAP price in each subplot.

compared to the base case. Similarly, the appliance cost of Case-I and Case-II, and Case-III and Case-IV are same i.e. appliance cost with and without combined HVAC and appliance optimization are the same. This indicates that HEMS schedule appliances in a similar pattern with or without co-optimization. The HEMS saving from appliance scheduling for January 2014 is approximately 41% for Cases I-II and approximately 28% for Cases III-IV whereas for January 2017 is approximately 20% for Cases I-II and approximately 16.5% for Cases III-IV. The appliance power for 7th January 2014 are presented in dashed purple line in Fig. 3.5.

As the appliance loads are shifted to the lower price hours from higher price hours

Table 3.3. Winter months electricity cost

Cases	2014			2017		
	HVAC (\$)	Appliance (\$)	Total (\$)	HVAC (\$)	Appliance (\$)	Total (\$)
Base	58.08	125.98	184.06	27.18	36.54	63.72
Case-I	66.36	74.75	141.11	27.9	29.66	57.56
Case-II	70.95	74.32	145.27	28.8	29.23	58.03
Case-III	67.97	90.93	158.9	27.52	30.54	58.06
Case-IV	70.12	90.75	160.87	28.85	30.36	59.21

to reduce cost, such as shifting of the appliance loads, in fact, decreases the heat gain from the appliances in high price hours. To compensate for the reduction of the heat gain from appliances, the house actually uses more HVAC energy during the high price period to maintain the consumer comfort. For winter months, the HVAC cost increased for Cases I-IV compared to the base case. It is noteworthy that though the HVAC cost increased, the overall bill decreased with the use of proposed HEMS. HVAC power, represented by a dashed blue line in Fig. 3.5, shows that the HVAC energy consumed during high price period (7 A.M - 12 P.M) is higher for Case I, III-IV compared to the base case thereby increasing the HVAC cost. Similarly, we also observed that the combined scheduling of HVAC and appliances with HVAC model (3.2) in Case-I and Case-III decreased the HVAC cost compared to independent scheduling in Case-II and Case-IV. This can be attributed to the improvement in the HVAC model with consideration of the appliance heat gain.

The temperature setpoint, as well as room temperature for Case-III and Case-IV are presented in Fig. 3.6. The HEMS normally sets the temperature setpoint to the minimum allowable temperature and performs pre-heating of the house before a high price period to save the HVAC energy consumption and reduce electricity bill. In the case of Case-III

with combined scheduling, the HEMS can accurately predict the setpoint temperature compared to Case-IV with independent scheduling. Thus, the room temperature follows the setpoint temperature more closely in Case-III compared to Case-IV. During the morning hours, the HEMS schedules the minimum allowable setpoint for both cases.

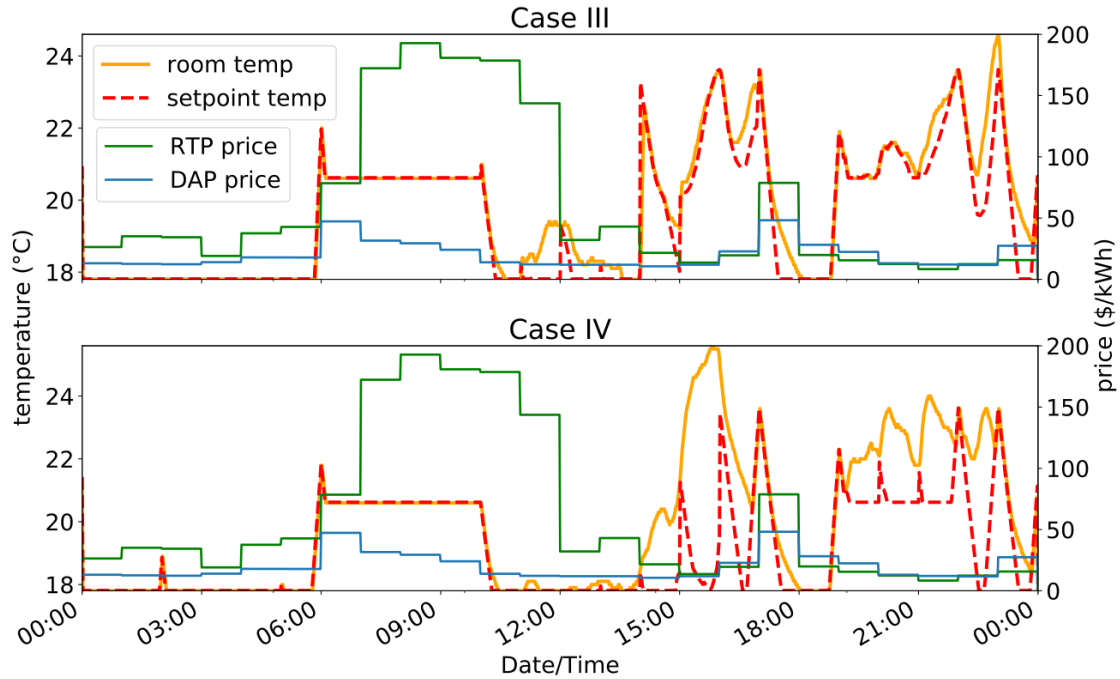


Figure 3.6. Comparison of the room temperature and setpoint for Case-III and Case-IV for January 7, 2014.

3.7.2 Summer Months

The EnergyPlus house model was simulated for the months of June-August for training the HVAC model for the summer months. The setpoint temperature of the building model was set to 23°C. Similar to winter months, the appliances schedule and heat gain were defined according to [52] for the summer months as well. The linear regression model and the least square estimation technique were used for computing the summer HVAC coefficients. The summer HVAC coefficients is presented in Table 3.2.

Table 3.4. June 2008 electricity cost

Cases	HVAC (\$)	Appliance (\$)	Total (\$)
Base	28.66	108.89	137.55
Case-I	15.19	78.82	94.01
Case-II	16.01	80.23	96.24
Case-III	16.22	85.02	101.24
Case-IV	16.92	85.71	102.63

For the month of June 2008, the HEMS with co-optimization of HVAC and appliance in Case-I and Case-III were able to save more compared to Case-II and Case-IV with independent optimization respectively as shown in Fig. 3.5. Similar to January 2014, HEMS saving can be further improved with more accurate price information as indicated by increased saving in Case-I compared to Case-III.

The HVAC cost, appliance cost, as well as total electricity cost for June 2008 is presented in Table 3.4. In contrast to winter months, there was notable saving in HVAC cost for all cases I-IV compared to the base case. Unlike winter months, for summer months, the scheduling of appliances away from the high price hours reduces the heat gain of appliances thereby reducing the AC energy consumption during high price hours to maintain the consumer comfort. Thus, we can see the saving in AC as well as appliances scheduling for the summer months.

3.8 Conclusion

This work presents a smart HEMS with the integrated HVAC and appliance scheduling to properly evaluate the performance of the HEMS. Such combined scheduling of HVAC and appliances in the HEMS ensures that the internal gain of the appliances is effectively considered during scheduling. Similarly, HEMS considers the comfort of the

consumers while scheduling appliances and HVAC setpoints to minimize the total electricity cost. Furthermore, incorporating a detailed thermal model of the residential building helps in proper evaluation of the HEMS performance. The simulation results demonstrate that HEMS reduced the total cost by approximately 9-14% though the cost of HVAC increased in the winter months. For the summer months, the HEMS reduced the total cost by approximately 27%. The proposed HEMS with combined scheduling of the HVAC and appliance improves resident's saving compared to the independent scheduling of HVAC and appliance.

CHAPTER 4 HIERARCHICAL CONTROL FRAMEWORK WITH NOVEL BIDDING SCHEME FOR RESIDENTIAL COMMUNITY ENERGY OPTIMIZATION

4.1 Background

Lack of coordination among the residential consumers participating in the DR programs causes more severe system peaks than found in normal operating conditions, as demonstrated in Chapter 2. Thus, the coordination among the participating DR resources is key and such coordination ensures the full potential benefits of the DR program are achieved. An incentive-based hierarchical control framework for coordinating and controlling a large number of residential consumers' appliances for achieving the desired benefits of the DR program is presented in this chapter ².

In the hierarchical framework, a number of residential consumers are grouped under a local controller (LC) , which controls the consumers' thermostatically controlled appliances (such as EWH and AC) during the DR event. The LC is also responsible for maintaining consumers' comfort, and rewarding them appropriately for their participation. Each LC submits a number of bids (consisting of reward and power limit) to the central controller (CC) . The CC selects the bid that optimally sets the demand limit for each LC. This framework also presents a demand reduction sharing technique among several LCs. The detailed description of the hierarchical framework along with a case study is

²The work presented in this chapter is a joint project with Dr. Zhen Ni and Priti Paudyal. I led the tasks associated with the formulation of the central controller (CC) including the design of the CC optimization formulation, the design of the bidding scheme for coordination of several local controllers (LCs) as well as collecting the relevant data for this work. Priti was in-charge of all works related to LC formulation which included incorporating appliance models and associated comfort, design of continuous reward structure, formulation of the LC optimization problem. We combinedly performed the case-study simulation and analysis of the results.

presented in this chapter.

4.2 Related works

In recent years, various energy optimization algorithms and approaches are proposed in the literature. In [55], a heuristic combinatorial optimization algorithm was proposed for load-leveling and demand reduction. An approximate dynamic programming approach was proposed in [56] to solve the energy optimization problem in a microgrid. A neural network was used in [57] to optimize data center operation and save energy and money. The authors in [58] used deep reinforcement learning to perform the online optimization of schedules for building energy optimization. In [55]–[58], the focus was on the energy optimization for non-residential sectors only, and so appliance level control was not implemented.

Similarly, different control frameworks for smart communities and energy districts have been studied in the literature. In [59], a novel cooperative distributed energy scheduling algorithm for a smart grid was proposed. This distributed algorithm minimized the total system day-ahead operating cost by optimally scheduling the charging/discharging of energy storage devices, and the output of conventional generators. Similarly, in [60], authors investigated a contribution-based energy allocation policy for trading energy among microgrids. A distributed model predictive control (MPC) framework aggregated thermostatically controlled loads, such as electric water heaters (EWH) and air conditioners (AC), to provide ancillary services is proposed in [61]. A Stackelberg game approach is introduced in [62] for energy sharing management within a microgrid with PV prosumers. Authors in [63] discussed a centralized MPC, and the

authors in [64] and [65] proposed a distributed MPC for coordination of networked microgrids to balance supply and demand. In [66], a stochastic bi-level framework is proposed to coordinate microgrids, as well as consider the stochastic nature of renewable energy. The research in this literature [59], [60], [63]–[66] introduced novel control frameworks focusing on energy balance within and between microgrids by optimally scheduling generation, storage, and/or flexible loads. Harnessing the market-level economic benefit from the residential demand reduction while considering both detailed appliance models and consumer incentives is not addressed in any single method [59]–[66].

Demand reduction for aggregated load demand has also been investigated in the literature. In [23], a distributed direct load control scheme was proposed for large-scale residential demand management, where the overall control was divided among each building's energy management controller (EMC). The EMC in each building was responsible for scheduling appliance operations to meet the local power consumption target. The work in [24] presented a bi-level coordinated optimization strategy to reduce the peak load demands considering online DR potential (DRP). Though aggregated load control was proposed in [23], [24], they did not provide rewards to the residential consumers for their participation. Similarly, in [25], a for-profit aggregator-based DR program was proposed which scheduled residential appliances maintaining the consumer preferences. Only non-thermal appliances were considered, and the potential privacy concerns in this centralized framework were not discussed. In [67], a decentralized approach to manage residential loads was proposed where an aggregator attempts to maximize profits, and consumers minimize costs in response to time-varying prices. The

load aggregator further offers additional incentives to reduce the system overload.

Wang et al. [68] investigated the case studies of several electric utilities DR programs and analyzed the effects of different incentives in the success and scalability of smart grid DR programs. In [69], the authors investigated the financial incentives essential to encourage plug-in hybrid electric vehicle owners to participate in demand reduction events. A framework for the incentive-based residential demand aggregation was proposed in [26]. Thermostatically controlled appliances, such as EWH and AC, were considered and a concept of comfort indicator (CI) was introduced to account for the consumers' discomfort. Although the authors considered consumer comfort and incentivized the participating consumers in [26], coordination mechanisms to address the sharing of demand reduction among the aggregators were not incorporated. Moreover, the change in the load profile considering a longer time horizon (e.g., rebound effect) was not presented.

Our previous work in [70] presented an early demonstration of incentive-based home energy optimization with DRPs for a small 20-house system. The demand reduction events were in the scale of 20–30 kW for a 30 minute reduction period. There was not a connection with the electric utility or bulk power market, and the impact after the demand reduction period ended was not analyzed. The demand reduction contribution of each local area may not be fair because each local controller was not able to provide any preferred demand limit. This motivated us to investigate new designs of demand allocation for large-scale residential energy optimization, consider the rebound effect after the demand reduction period, and analyze the benefits for the bulk power market and electric utility. Furthermore, the discrete reward structure in [70] causes computational intractability when the scale of system increases, which inspired the authors to explore the

alternative continuous reward structure in this work that scales very well with increased system size.

4.3 Proposed Work

There are several key elements in residential energy optimization research, such as proper allocation or coordination of the demand reduction, reward distribution for incentivizing the consumers, identification of the demand reduction period, analysis of the market-level economic benefit of such demand reduction, and consideration of detailed residential appliance models. However, in the literature, there is not a single framework that incorporates each of these key elements to harness the economic benefits of residential DR in a realistic, market-level scale. Thus, this work proposes a new integrated hierarchical control framework for residential energy optimization, coordinating and controlling large electric appliances and considering residents' comfort and supplying rewards.

In this chapter, a novel bidding scheme to coordinate the demand reduction events between a CC, several LCs, and a number of residential consumers in a hierarchical framework is presented. Similarly, a new continuous reward (incentive) for participating consumers based on their comfort level is designed. Furthermore, potential market-level benefits of the residential demand reduction in terms of change in locational marginal price (LMP) are quantified.

4.4 Appliance Model

In this section, the appliance models, consumer preferences, and CI are explained in detail. The home electric appliances considered here are the thermostatically controlled

appliances, i.e., AC and EWH. The reasons for choosing AC and EWH are (i) they are major power consuming appliances in residential buildings, and (ii) their high thermal inertia makes them suitable for DR because they can store thermal energy for some time. These appliances function to maintain the room and water temperatures within user-specified ranges. There are various types of models for AC and EWH as presented in the literature [71]–[77]. In this work, the models from [77] are considered. Although not presented in this work, the work is easily extendable to heating loads.

4.4.1 Air Conditioner Model

An AC consumes its rated power when turned ON. The AC is turned ON and OFF by the thermostat that controls the building temperature. The room temperature varies within a given deadband around the thermostat setpoint temperature. The ON/OFF status of the AC for cooling purpose follows the following pattern: when the room temperature increases above the upper bound, the AC is turned ON and consumes the rated power until the room temperature reaches the lower bound. After the temperature strikes the lower bound, the AC is turned OFF and does not consume power until it reaches the upper bound again. The estimation of room temperature developed in [77] is presented in Eq. (4.1). The AC model depends on the room temperature of the previous time step, outdoor air temperature, AC capacity, AC status, and the house parameters (e.g., house size, size of south-facing windows, and the number of occupants) to calculate the heat gain.

$$T_{i+1} = T_i + \Delta t \cdot \frac{G_i}{\Delta c} + \Delta t \cdot \frac{C_{AC}}{\Delta c} \cdot W_{AC,i} \quad (4.1)$$

where, T_i represents the room temperature in time slot i ($^{\circ}\text{F}$), Δt is length of time slot i (hour), G_i is heat gain rate of the house during time slot i (Btu/h), C_{AC} is cooling/heating capacity (Btu/h), Δc is energy needed to change the temperature of the air in the room by 1 $^{\circ}\text{F}$ (Btu/ $^{\circ}\text{F}$), $W_{AC,i}$ is status of the AC unit in time slot i (0=OFF, 1= ON).

4.4.2 Electric Water Heater Model

The EWH functions similar to the AC. The heating coils operate at the rated power when the water temperature drops below the defined lower bound. The heating coils turn OFF when the water temperature reaches the upper bound and turn back ON only after the water temperature decreases to the lower bound. The hot water temperature is estimated according to the revised model from [77], as presented by Eq. (4.2).

$$T_{outlet,i+1} = \frac{T_{outlet,i}(V_{tank} - fr_i \cdot \Delta t)}{V_{tank}} + \frac{T_{inlet} \cdot fr_i \cdot \Delta t}{V_{tank}} + 1 \frac{\text{gal}}{\text{lb}} \left[P_{WH,i} \cdot 3412 \frac{\text{Btu}}{\text{kWh}} - \frac{(T_{outlet,i} - T_i)}{R_{tank}} \cdot A_{tank} \right] \cdot \frac{\Delta t}{60 \frac{\text{min}}{\text{h}}} \cdot \frac{1}{V_{tank}} \quad (4.2)$$

where, $T_{outlet,i}$ represents hot water temperature in time slot i ($^{\circ}\text{F}$), T_{inlet} is temperature of inlet water ($^{\circ}\text{F}$), T_i is room temperature ($^{\circ}\text{F}$), $P_{WH,i}$ is power consumed by water heater (kW), fr_i is hot water flow rate in time slot i (gpm), V_{tank} is volume of the tank (gallons), A_{tank} is surface area of the tank (ft^2), R_{tank} is heat resistance of the tank ($^{\circ}\text{F} \cdot \text{area} \cdot \text{h}/\text{Btu}$), Δt is duration of each time slot (minutes).

4.4.3 Consumer Preferences and Comfort Indicator

The smart AC and EWH maintain the room and the water temperatures, respectively, within a certain range. The temperature ranges for the operation of these appliances are user-defined. Thus, the upper and lower temperature bounds for the normal

operation of both appliances are the preferences of the consumer. In addition to the normal operating temperature range, the maximum and minimum allowable temperatures during the time of demand reduction are also user-defined.

A consumer's comfort level for the thermostatically controlled loads is mainly associated with the temperature. So, the consumer's thermal comfort level is measured in terms of CI [26] as represented by Eq. (4.3).

$$CI_a = \left| \frac{2T_a - T_a^{low} - T_a^{high}}{T_a^{high} - T_a^{low}} \right| \quad (4.3)$$

where, for appliance a (e.g., AC or EWH), T_a is the instantaneous temperature, T_a^{high} is the upper temperature bound for normal operation, and T_a^{low} is the lower temperature bound for normal operation. The distance between the current temperature and the defined ideal temperature is determined by CI_a . The ideal temperature here is the mean of the upper and lower temperature (consumer's preferences) for normal operation. Since CI is defined as the absolute value, it is always a positive value. If the CI is greater than 1, then it indicates that the temperature is beyond the normal operating range. Meanwhile, the CI also helps in choosing the appropriate appliance among the available appliances for energy optimization. Eq. (4.3) shows that the smaller the value of CI, the greater the potential of the smart appliance to contribute to the demand reduction.

Here, let us consider an example of a consumer with an AC unit. The consumer prefers the temperature of T_{AC}^{low} to T_{AC}^{high} for the normal operation of the AC. The temperature for normal operation of AC means that consumer's room temperature is maintained within T_{AC}^{low} to T_{AC}^{high} at all times, except for demand reduction periods. However, the AC may be turned off to reduce the power consumption during a demand

reduction period. In doing so, during the summer, the room temperature may increase above T_{AC}^{high} . It is important to indicate the extent up to which the temperature can increase or decrease for participating consumers. Thus, the minimum and maximum allowable temperature, T_{AC}^{min} and T_{AC}^{max} , respectively, are required from the consumer to maintain their comfort during the demand reduction period (with $T_{AC}^{min} \leq T_{AC}^{low}$, and $T_{AC}^{max} \geq T_{AC}^{high}$). The values of T_{AC}^{min} and T_{AC}^{max} bound the CI, and hence the consumer reward.

Furthermore, the consumer preferences for the temperature also signify their willingness to compromise. If the consumer is more concerned about being comfortable than receiving more reward, then one will prefer a smaller range of allowable temperatures. Inversely, the consumer will opt for a larger range if they are more willing to compromise. The reward scheme based on CI is described in the next section.

4.5 Hierarchical Control Framework

The proposed framework is from the perspective of an electric utility, where the main goal is to fulfill the demand reduction by providing minimum rewards to the consumers, while also ensuring consumer comfort during the demand reduction. The proposed hierarchical control framework consists of three layers. As shown in Fig. 4.1, the bottom layer comprises the communication between residential consumers and LCs, the interaction between the LCs and the CC constitutes the middle layer, and the top layer interfaces the CC and electricity market.

The privacy of consumer data is a major concern for the consumers participating in demand reduction events. The proposed hierarchical framework ensures that the consumer data (individual appliance usage profile and preferences) are shared only with the LCs,

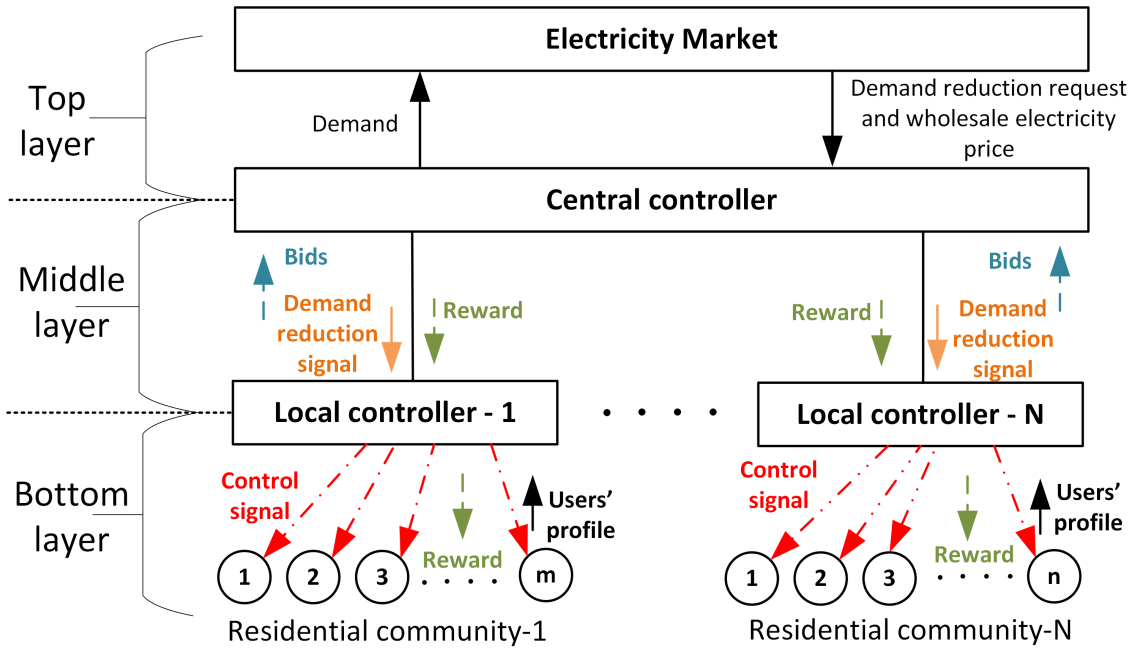


Figure 4.1. System block diagram of the proposed hierarchical control structure for residential community energy optimization. It shows the components of the proposed hierarchical framework, along with the information exchange between the components, represented by arrows.

minimizing such privacy concerns. The utility (CC) has access only to the aggregated power consumption profile. On the other hand, the proposed framework also assures scalability with a large number of residential consumers. We assume that there is no significant communication delay for data exchange between layers. The design of a new continuous reward, the residential community, LC, CC, and the impacts on the electricity market are explained in detail in this section.

4.5.1 Novel Continuous Reward Structure

A new continuous reward scheme for the demand reduction event is designed, where consumer reward is directly proportional to the CI. The first advantage of the continuous reward (compared to the discrete reward levels in [26]) is that it provides fairness among participating consumers. As reward is proportional to the CI, a consumer

with higher discomfort receives a higher reward. Second, the continuous reward reduces the optimization complexity by using continuous decision variables, as opposed to integer variables as in [26], [70]. The continuous reward is expressed as Eq. (4.4), which is used in the optimization.

$$R_{a,t} = r \cdot CI_{a,t} \cdot P_a^{rated} \cdot \Delta t \quad (4.4)$$

where, for appliance a at time t , r is the reward rate ($\$/\text{kW} \cdot \text{min}$), $CI_{a,t}$ is the comfort indicator, P_a^{rated} is the rated power (kW), and Δt is the time interval considered (min).

After the optimization is performed, a post-processing step is performed to calculate the actual reward given to consumers. Here, the actual reward amount is provided to consumers only when CI exceeds 1 (i.e., their comfort is violated), as shown in Eq. (4.5).

$$Reward_{a,t} = \begin{cases} 0, & \text{if } CI_{a,t} \leq 1 \\ r \cdot CI_{a,t} \cdot P_a^{rated} \cdot \Delta t, & \text{if } CI_{a,t} > 1 \end{cases} \quad (4.5)$$

This implies that a consumer will receive reward for time step t if the temperature at that time is beyond the normal operating range. Based on the preferred temperature settings of participating consumers, the CI is calculated. It should be noted that although it seems that selecting a small range for the temperature preference would provide the higher reward, the optimization selects appliances to contribute in the demand reduction that requires minimal reward (as a main objective for the proposed framework is to provide the minimum reward for a given demand reduction). Thus, in fact, the appliances having higher temperature range have higher chances to participate in the optimization process and receive rewards.

4.5.2 Residential Community

Each house of the residential community is modeled with thermostatically controlled loads, explained in Section 4.4, and a non-controllable base load. The base load is created using the queue model introduced in [14], where each home has a unique time-varying load that statistically represent a known system load curve. A residential community comprising of several homes is linked with an LC and participate in the incentive-based demand reduction events. Each consumer shares their preferences and load information only with their corresponding LC.

4.5.3 Local Controller Design

Each LC is responsible for coordinating the thermostatically controlled appliances (AC and EWH) of a residential community during demand reduction events while considering residential consumer comfort. The LCs have access to the local residential consumer information regarding thermal appliance status and preferences. The algorithm of an LC is presented in Algorithm 2.

Algorithm 2: LC algorithm

- 1 Receive request from CC to submit bids ($b = 1, \dots, B$)
 - 2 To generate each bid (b):
 - a. Minimize Eq. (6) subject to Eqs. (1), (2), and (7)–(9), while keeping power consumption within ($p_{i,b}$)
 - b. Obtain control signals ($\delta_{a,t}$) to optimize the operation of each consumer appliance ($a = 1, \dots, A$) for the given power consumption limit ($p_{i,b}$)
 - 3 Submit the bids ($b = 1, \dots, B$) to CC
 - 4 Wait for CC to complete Steps 3–6a in Algorithm 3
 - 5 Receive selected bid from CC (R_i, PL_i)
 - 6 Based on the selected bid, dispatch:
 - a. Control signal ($\delta_{a,t}$) to each consumer appliance ($a = 1, \dots, A$)
 - b. Calculate reward for each consumer ($Reward_{a,t}$) using Eq. (5)
-

For a demand reduction event, the CC sends a demand reduction signal and requests each LC to submit their bids to participate in the event. On receiving the signal from the CC, each LC performs optimization for several demand reductions (i.e., different power reduction amounts) to generate respective bids. Each bid compromises a reward amount corresponding to a certain demand reduction. For each bid, an LC performs a MILP optimization to calculate the optimal reward for a specific power limit. The main objective of the LC optimization is to minimize the total reward for each bid. Mathematically, the objective of LC can be expressed by Eq. (4.6).

$$RW_{i,b} = \min_{\delta_{a,t}} \sum_{t=1}^{\tau} \sum_{a=1}^A r \cdot CI_{a,t} \cdot P_a^{rated} \cdot \Delta t \quad (4.6)$$

Subject to

$$CI_{a,t} = \left\lfloor \frac{2T_{a,t} - T_a^{low} - T_a^{high}}{T_a^{high} - T_a^{low}} \right\rfloor, \quad \forall t = 1, \dots, \tau \quad (4.7)$$

$$\sum_{a=1}^A P_a^{rated} \cdot \delta_{a,t} + P_{i,t}^{base} \leq p_{i,b}, \quad \forall t = 1, \dots, \tau \quad (4.8)$$

$$T_a^{min} \leq T_{a,t} \leq T_a^{max}, \quad \forall t = 1, \dots, \tau \quad (4.9)$$

and other appliance model constraints including Eqs. (4.1) and (4.2), and AC heat gain equations from [77]. Eq. (4.7) calculates the CI for each consumer, Eq. (4.8) ensures that the total power consumption of the residential consumers under each LC does not exceed their bidding power, and Eq. (4.9) ensures that the temperature does not exceed the resident defined minimum and maximum temperature.

Here, $RW_{i,b}$ is the continuous reward corresponding to bid b for LC i , $\delta_{a,t}$ is the ON/OFF status of appliance a at time t , $T_{a,t}$ is the temperature of to appliance a at time t ,

A is the total number of appliances under LC i , τ is the total time considered, $P_{i,t}^{base}$ is the total base power of LC i at time t , $p_{i,b}$ is the power limit corresponding to bid b for LC i , and T_a^{min} and T_a^{max} are the minimum and maximum allowable temperature for the operation of appliance a , respectively. The main decision variable for optimization is $\delta_{a,t}$.

To illustrate the LC bidding strategy, let us consider LC X preparing B bids. For the first bid, LC X minimizes consumer reward $RW_{X,1}$ considering consumer comfort for a particular demand reduction $p_{X,1}$. After optimization, LC X prepares the first bid as $[RW_{X,1}, p_{X,1}]$. Similarly, LC X arranges the rest of the $B - 1$ bids. The LC then submits the B bids $([RW_{X,1}, p_{X,1}], \dots, [RW_{X,B}, p_{X,B}])$ to the CC.

Let us assume the CC notifies LC X that bid i ($[RW_{X,i}, p_{X,i}]$) is selected among the submitted bids, i.e., the demand limit for the LC is $p_{X,i}$. The LC then dispatches the control signal to each resident appliance based on bid B , and distributes reward ($RW_{X,i}$) to the consumers for their participation.

4.5.4 Central Controller Design

The CC is responsible for coordinating several LCs for residential community energy optimization when demand reduction is considered appropriate for the system (technically or economically). The CC can be represented by the utility itself, or another independent entity. The algorithm for the CC is presented in Algorithm 3.

On receiving the demand reduction request signal from the market, the CC requests each LC to submit respective bids. After the LCs submit their bids, the CC performs a MILP optimization to select the optimal bid from each LC to minimize the total cost of performing the demand reduction. The optimal bid for each LC comprises the total

Algorithm 3: CC algorithm

- 1 Receive demand reduction request signal from the market
 - 2 Request all LCs to submit their bids
 - 3 Gather all bids ($b_i = 1, \dots, B_i$) from the LCs ($i = 1, \dots, N$), i.e, Steps 2 and 3 of Algorithm 2
 - 4 Calculate optimal bid for each LC by minimizing Eq. (10) subject to constraints (11)–(14)
 - 5 Obtain optimal values for $\omega_{i,b}$ to determine reward R_i and demand limit PL_i for each LC
 - 6 Dispatch:
 - a. Optimal bids to each LC, i.e., set power limit (PL_i) to each LC and distribute reward (R_i)
 - b. Inform market of the reduced demand
-

demand reduction of each LC, and the corresponding reward that each LC calculates for its customers' participation. The CC then sends the selected optimal bid for each individual LC with information about the demand reduction and reward to each LC.

The objective of the CC is to minimize the total reward payment to the residential consumers while satisfying the required demand reduction. Mathematically, the objective of the CC can be expressed as Eq. (4.10).

$$\min_{\omega_{i,b}} \sum_{i=1}^N R_i \quad (4.10)$$

Subject to:

$$\sum_{b=1}^B \omega_{i,b} = 1 \quad \forall i = 1, \dots, N \quad (4.11)$$

$$R_i = \sum_{b=1}^B \omega_{i,b} \times RW_{i,b} \quad \forall i = 1, \dots, N \quad (4.12)$$

$$PL_i = \sum_{b=1}^B \omega_{i,b} \times p_{i,b} \quad \forall i = 1, \dots, N \quad (4.13)$$

$$\sum_{i=1}^N PL_i \leq P_{limit} \quad \forall i = 1, \dots, N \quad (4.14)$$

Here, R_i is the optimal reward for LC i , $\omega_{i,b}$ is a binary decision variable corresponding to bid b of LC i , PL_i is the optimal demand limit for LC i , P_{limit} is the total power limit for all LCs, and N is the total number of LCs. Eq. (4.11) ensures that only one bid is selected from each LC, Eq. (4.12) provides the selected reward for each LC, Eq. (4.13) computes the selected power limit of each LC, and Eq. (4.14) guarantees that the total power consumption of all residential consumers under all LCs is within the prescribed total limit.

To illustrate the bid selection process, let us consider a CC with two LCs (X and Y). Considering each LC submits B bids i.e., $([RW_{X,1}, p_{X,1}], \dots, [RW_{X,B}, p_{X,B}])$ and $([RW_{Y,1}, p_{Y,1}], \dots, [RW_{Y,B}, p_{Y,B}])$, the CC selects the optimal bid for each LC that satisfies the power limit (P_{limit}) at the minimum reward. Suppose the optimal bids are bid i for LC X ($[RW_{X,i}, p_{X,i}]$), and bid j for LC Y ($[RW_{Y,j}, p_{Y,j}]$). The CC then sends the corresponding demand limits ($p_{X,i}$ for LC X and $p_{Y,j}$ for LC Y) and the reward ($RW_{X,i}$ and RW_j) to the respective LCs.

4.5.5 Impacts on Electricity Market

In this work, the method employed in [78] is used to emulate the LMP of an actual U.S. electricity market. In [78], an unsupervised learning technique classifies real generators based on the offer data submitted by the generators to the PJM market. Realistic market-based generator cost curves are obtained by fitting the quadratic cost curve for each generator cluster. These market-based cost curves are used for the

calculation of optimal power flow (OPF) , providing the LMP of each bus of the system that represents the actual PJM energy market.

In our work, LMP is calculated for two cases: (i) with demand reduction, and (ii) without demand reduction, for each hour. The reduction of LMP of each bus, as well as the total utility savings for each hour, are then computed to see the economic impact of the demand reduction. Only those hours in which there is a significant reduction in the LMP and significant utility savings considering the reward are considered appropriate demand reduction periods. On selecting the suitable demand reduction period, the market then sends information about the reduction in LMP and requests for the demand reduction to the CC. After the CC performs the demand reduction, it sends the information on reduced demand to the market.

4.6 Simulation Setup

The RBTS IEEE-6 bus system [79], a test case shown in Fig. 4.2, is considered in this work. This test case has 6 buses with a total generation capacity of 240 MW. The bus loads are scaled according to PJM load to replicate the actual behavior of the PJM electricity market, as described in [78]. In this work, it is assumed that a single utility supplies electricity to all loads of each of the 6 buses. The utility payment, calculated based on the LMP calculated by OPF, is determined before and after demand reduction to evaluate the economic benefit of the demand reduction. In this work, 30% of the total load is considered to be residential [80]. Among the residential load, the utility assumes that 20% of the loads can be controlled and thus calculates the demand reduction for each hour. This amount of load, which is approximately 6% of the total demand, was chosen as

it represents the amount of demand used in actual DR events in PJM [81].

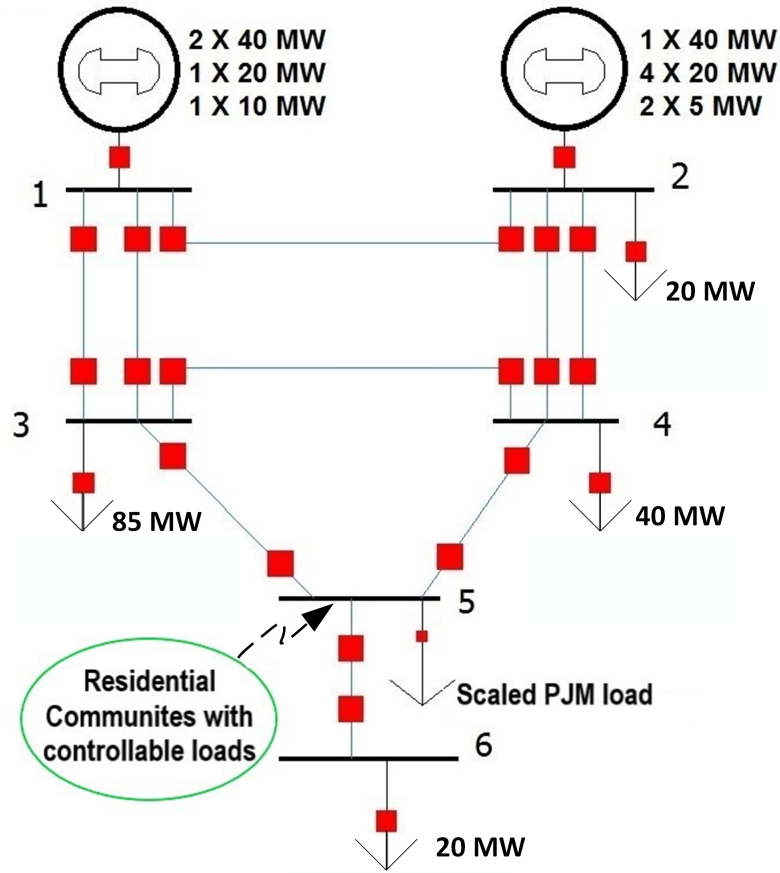


Figure 4.2. RBTS system with the location of the loads and maximum generation limits of the system [82].

The residential houses are assumed to be on bus 5 of the test system. A CC with 60 LCs, with varying numbers of homes between 10 to 30 under each LC, are considered in the case study. It is assumed that each LC generates 7 bids by keeping its total power consumption within 70% to 100% of its peak power demand, with a step change of 5%. Altogether 1,200 residential houses were considered in this study.

The consumer preferences for the temperatures are randomly generated within a specific range. The lower and upper temperature bounds for the normal operation of the

AC are randomly selected within 68°F to 70°F and 73°F to 75°F, respectively. Similarly, the minimum and maximum allowable room temperatures are randomly chosen within 60°F to 65°F and 80°F to 84°F, respectively. Likewise, for the EWH the lower temperature and upper temperature for normal operation, and the minimum and maximum allowable water temperatures are randomly chosen within 105°F to 108°F, 118°F to 122°F, 90°F to 103°F, and 125°F to 130°F, respectively. Note that these are typical realistic values, and each individual consumer has different settings. The initial room and water temperatures are randomly initialized within 69°F to 74°F, and 110°F to 118°F, respectively. The initial status for all the appliances are randomly set as 1 (ON) or 0 (OFF). The reward rate is considered as 0.04 \$/kW · min [26].

A hot summer day (7/1/2014) is chosen to conduct the demand reduction. The realistic residential water use schedule for the EWH model is generated from [83], whereas the outdoor temperature for an AC model is obtained from typical meteorological year (TMY3) weather format of Chicago, IL, to correlate with the PJM market data. Unique time-varying base load was created for each house using the $M_t/G/\infty$ queue model from [14]. The queue model statistically creates individual house loads based on a reference load derived from a known system load curve. For this simulation, load from PJM for July 1, 2014 [84], was scaled down to the reference load representing a single household using a minimum and maximum load of 100 W and 5000 W, respectively, according to [14] for use in the queue model. The rest of the load on bus 5 of RBTS was scaled from the PJM load according to [78].

The simulation is performed using MATLAB R2017b and CPLEX 12.7.1. The relative MIP gap in CPLEX, a relative difference between the best bound and the found

feasible solution, is set as 10% for optimization in LC and default 0.01% for optimization in CC.

4.7 Result and Discussion

The savings to the utility due to the demand reduction in each hour of the simulation day (7/1/2014) is represented in Fig. 4.3, which is obtained from the OPF for the two cases of with and without demand reduction. From the figure, it can be seen that conducting demand reduction of approximately 1.2 MW from 2 to 3 pm in the afternoon could save \$39,359 and decrease the LMP from 294.11 \$/MWh to 80.62 \$/MWh. Due to network configuration and generator configuration (generator size and scheduling), there is no significant saving for conducting demand reduction for any other period. With this information, 2 to 3 pm on this day was chosen as the appropriate time to perform the demand reduction study.

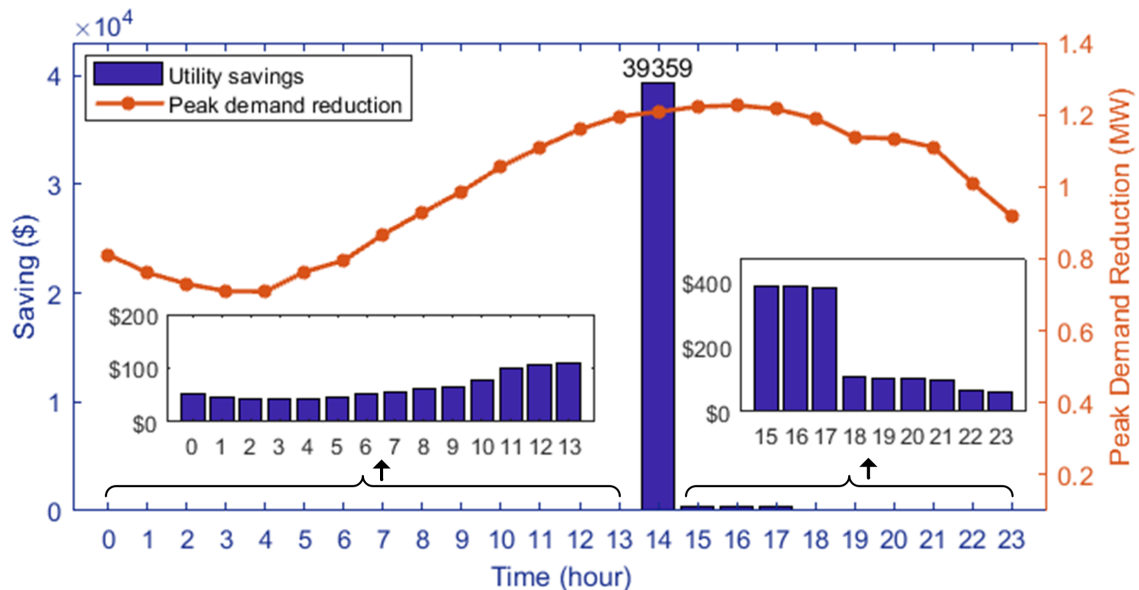


Figure 4.3. Total utility savings from demand reduction in each hour. The blue bar graph depicts the total utility saving each hour from the peak demand reduction, which is shown by the red curve.

The residential community load profile for the day without demand reduction, generated using the initial conditions and base load information explained above in Section 4.6, is shown in Fig. 4.4. This load profile represents the total load of the participating residential consumers only (the remaining load comes from the scaled PJM load). The demand reduction event period (2 to 3 pm) is marked within the black-dashed rectangle. The green curve represents the total load profile of the participating houses, i.e., the combination of base, AC, and EWH loads. The red curve represents the total base loads, which cannot be controlled. The blue curve represents the total AC and EWH loads, i.e., controllable loads for demand reduction.

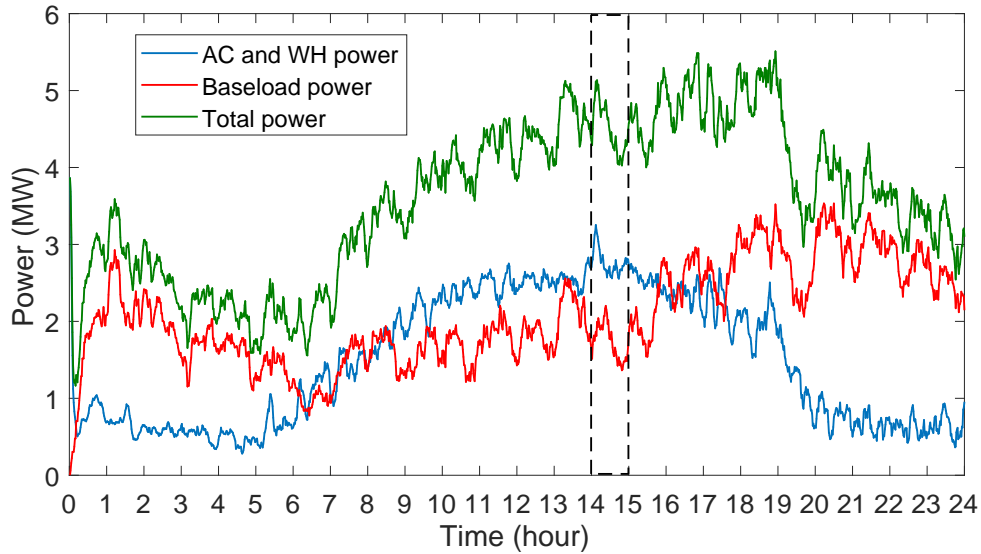


Figure 4.4. Normal load profiles for AC and EWH load, baseload, and total load. The one-hour interval within the black dashed rectangle represents the demand reduction period.

For the explanation of the bids from an LC during the demand reduction event, an example bid from LC-2, corresponding to 10 homes, is represented by Fig. 4.5. A total of $B = 7$ bids are offered, as explained in Section 4.5.3. The first bid is zero reward for zero demand reduction (i.e., the LC is not selected for demand reduction), while the last bid is

\$160.20 for 16.94 kW peak demand reduction. From the figure, it can be observed that the total reward increases with the increasing peak demand reduction. In this particular case of LC-2, for the last bid, the minimum and maximum rewards given to the consumers are \$0 and \$16.59, respectively. The consumers with higher priority for comfort (i.e., by selecting a smaller range of temperature), received lower rewards compared to consumers more willing to compromise.

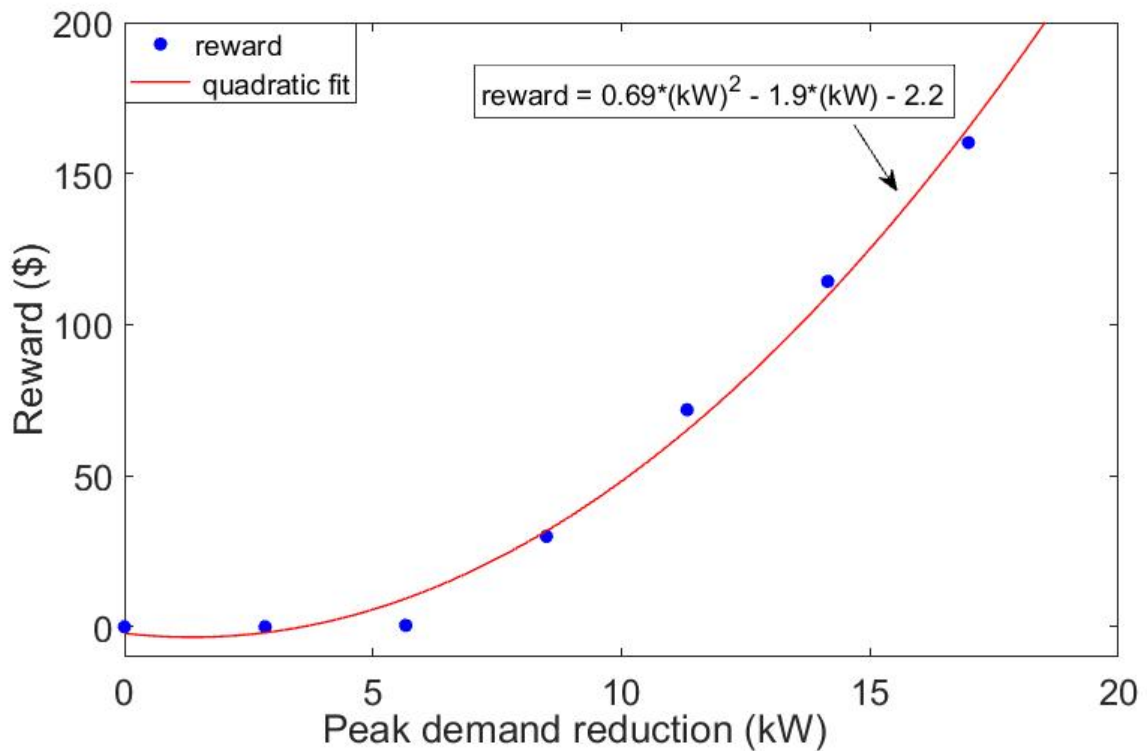


Figure 4.5. An example of different bids submitted by LC-2. The blue dots represent the reward calculated by LC-2 for different peak demand reductions, and the red curve represents the trendline for the reward variation with increasing demand reduction.

Several demand reduction cases from 0.4 MW to 1.2 MW peak demand reduction are considered. The results for total rewards distributed to the consumers by CC, as well as the mean and standard deviation of the reward distribution, are presented in Table 4.1. Considering Case-V, the total reward that the utility has to pay to the consumers is

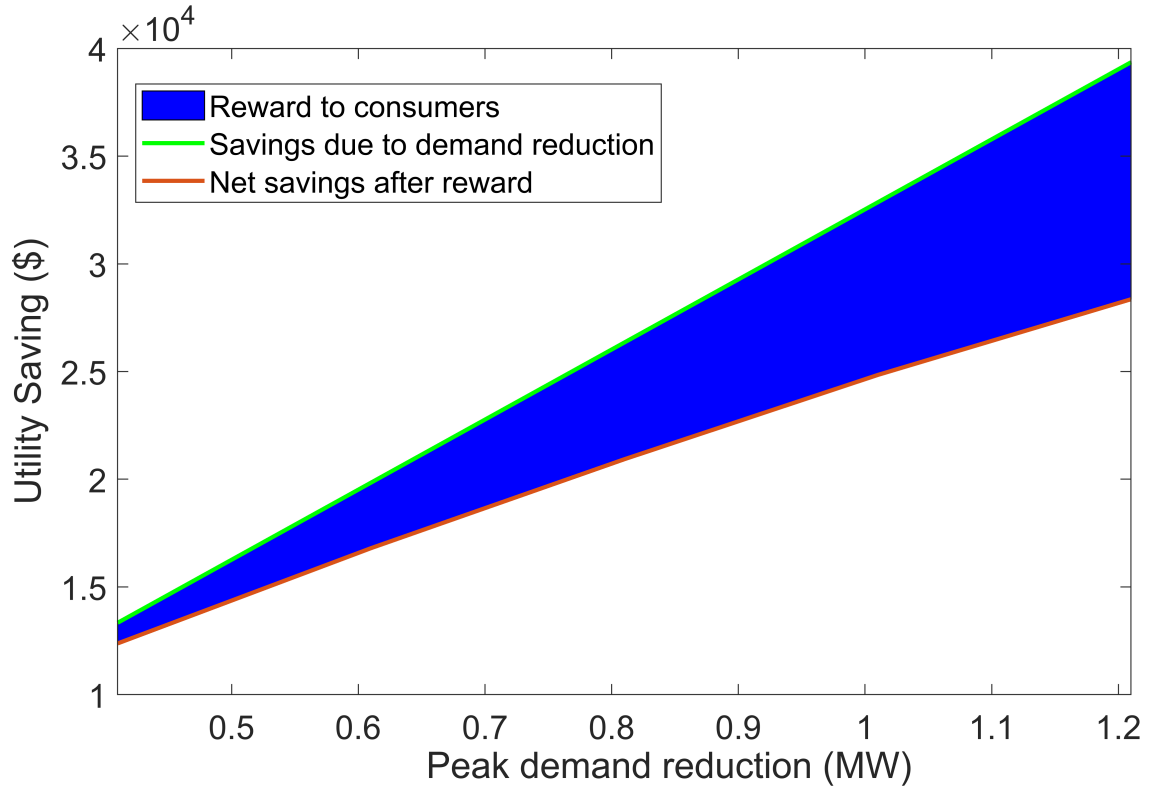


Figure 4.6. Total utility savings before and after rewards for different demand reductions. The upper line represents the total utility savings without considering reward, and the lower line represents the net utility savings after providing the consumer reward. The blue region between the lines represents the reward provided.

\$11,002 for 1.2 MW total peak demand reduction. In terms of \$/kW, it is 7.33 \$/kW, which means the utility pays \$7.33 on average for reducing 1 kW of peak demand. The minimum and maximum reward distributed to the consumers are \$0 and \$25.01, respectively, for the one-hour demand reduction. Moreover, the mean and standard deviation of the consumer reward is \$9.37 and \$7.75, respectively. From this table, it can be observed that the average and the standard deviation of the reward to the consumers increases with the increasing demand reduction.

Fig. 4.6 presents the net savings to the utility for different cases of demand reduction. For the case of 1.2 MW, after considering the reward provided to the residential

Table 4.1. Total utility reward and mean and standard deviation for consumer reward for different demand reduction cases

Case	Total peak reduction (MW)	Total utility reward (\$)	Average utility reward (\$/kW)	Mean of consumer reward (\$)	Standard deviation of consumer reward (\$)	Maximum consumer reward (\$)
Case-I	0.4	958.15	1.37	0.77	2.39	15.72
Case-II	0.6	3041.21	3.38	2.42	4.80	16.95
Case-III	0.8	5418.70	4.92	4.55	6.66	25.01
Case-IV	1.0	8012.40	6.16	6.91	7.46	25.01
Case-V	1.2	11002.51	7.33	9.37	7.75	25.01

consumer and the decrease in LMP after the demand reduction event, the total net savings of the utility is \$28,217. For other cases, assuming the utility savings from residential demand reduction is proportional to its contribution to the total demand reduction, the utility can have significant savings by conducting the residential demand reduction. In such cases though, the fraction of the total demand reduction is fulfilled by other resources (i.e., not through the hierarchical framework) to harness significant savings.

The residential consumers' load profile before and after demand reduction event is presented in Fig. 4.7. It can be seen that the load profile of the participating consumers during the demand reduction remains below the power limit set by the CC. After the demand reduction period, the peak load consumption compared to the baseline profile increases, indicating a rebound effect that can be observed. This rebound effect seen immediately after the end of demand reduction event is due to most of the residential appliances simultaneously starting after the demand reduction period ends to return towards the temperature bounds. However, this increased rebound did not cause significant additional costs to the utility, as it caused minimal increases in LMP compared to the savings during the demand reduction period.

Comparing the reward of the proposed framework with the rewards provided by existing utilities, Pacific Gas and Electric (PG&E) [85] offers 16.30 \$/kW, whereas

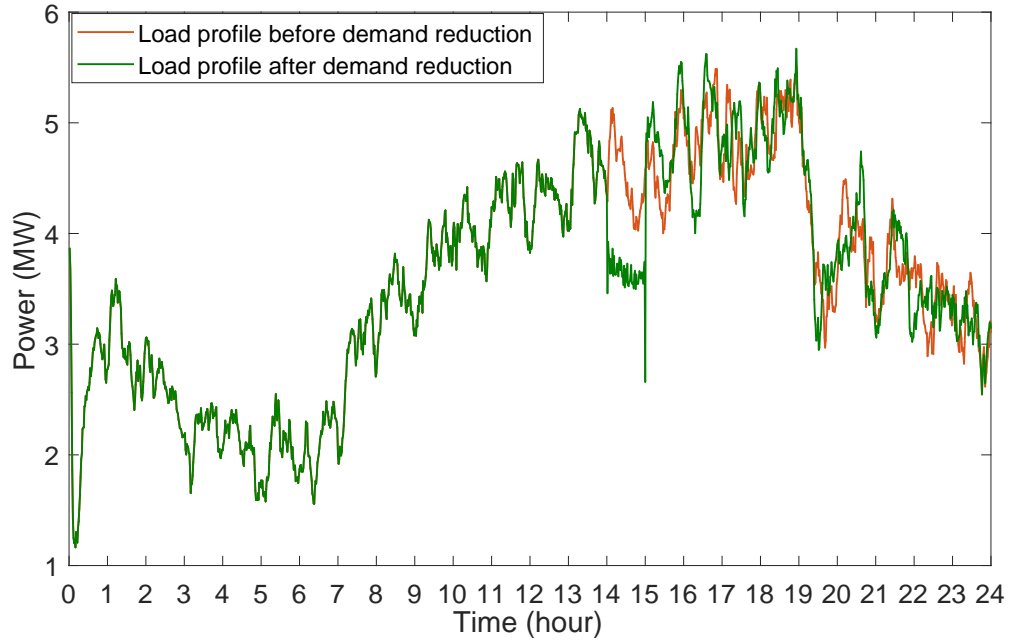


Figure 4.7. Load profile of the residential consumers before and after demand reduction event. The red line represents the load profile before demand reduction, and the green line represents the load profile after demand reduction.

Southern California Edison (SCE) [86] offers 16.78 \$/kW to third-party aggregators for the month of July. Based on these rates, the total reward would be approximately \$20,000 for 1.2 MW of the demand reduction. With the proposed framework, the total reward distributed among the consumers is \$11,002 for reducing 1.2 MW peak demand, which is significantly lower than the existing utility reward. The economic viability of the 0.04 \$/kW · min reward rate for motivating the consumer will be considered in future work.

4.8 Conclusion

This work presents a novel hierarchical framework for a large-scale residential energy optimization. The proposed hierarchical framework ensures algorithm scalability, as well as maintains the privacy of the residential consumers. The results presented show that both the consumers and the utility are benefited from the proposed incentive-based

energy optimization. From a consumer's perspective, the proposed reward is flexible, where one can choose to get more reward for providing thermal flexibility of appliances, or can remain within the desired comfort region receiving less reward. This is evidenced by the minimum and maximum reward consumers received in the results, i.e., \$0 and \$25. Additionally, consumer appliance usage and preference data are kept private within an LC, which ensures consumer privacy. On the other hand, the utility can save a large amount by conducting the demand reduction just for one hour, which is evident from the \$28,217 net savings shown in the result for reducing 1.2 MW peak demand. Furthermore, the load profile after the demand reduction event is analyzed to observe the rebound effect. The net saving of the utility is also calculated after considering the consumer reward and increase in LMP due to rebound peak.

CHAPTER 5 CONCLUSIONS

This research work presented a co-simulation framework tool for coupling EnergyPlus and GridLAB-D, an individual HEMS with integrated scheduling of HVAC and appliances, as well as hierarchical framework for controlling large number of residential appliances.

Controllers, such as HEMS and aggregators, can be easily incorporated into the co-simulation framework allowing design, testing, and validation of control algorithms for residential energy management while considering distribution impacts. The case study showed that greedy HEMS optimization based on the same pricing signals causes system peaks more severe than normal operating conditions. This showcases the need for the co-simulation framework presented in this work that models in detail many homes and verifies grid impacts, allowing for future Smart City simulations.

The detailed modeling of an individual HEMS with combined scheduling of HVAC and other appliances in co-simulation framework was also presented. Such combined scheduling of HVAC and appliances in the HEMS ensures that the internal gain of the appliances is effectively considered during scheduling. Similarly, HEMS also considered the residents' comfort while scheduling appliances and HVAC setpoints to minimize the total electricity cost. The case study demonstrated that the HEMS with combined scheduling of the HVAC and appliance improved resident's saving compared to the independent scheduling of HVAC and appliances.

The hierarchical framework for large scale residential energy optimization with bidding scheme ensures proper coordination of large number of residential appliances,

algorithm scalability, as well as maintains the privacy of the residential consumers. Also, both utility, as well as participating residents receives the economic benefits from the incentive-based residential optimization. From the consumers' perspective, the participating consumers are rewarded based on the thermal flexibility offered. The consumers can choose to receive higher reward for their flexibility or prefer to remain within their thermal comfort for lesser reward. The variation of reward in the case study (\$0 to \$25) represents the consumers' willingness and flexibility. On the other hand, utilities also gain a net saving (considering the consumers' incentive as well as change in LMP due to rebound effect) from the aggregate demand reduction of residential consumers' demand as evident from \$28,217 net savings for reducing 1.2 MW in the case study.

REFERENCES

- [1] N. Bassamzadeh, R. Ghanem, S. Lu, and S. J. Kazemitabar, "Robust scheduling of smart appliances with uncertain electricity prices in a heterogeneous population," *Energy and Buildings*, vol. 84, pp. 537–547, 2014.
- [2] H. T. Haider, O. H. See, and W. Elmenreich, "A review of residential demand response of smart grid," *Renewable and Sustainable Energy Reviews*, vol. 59, no. C, pp. 166–178, 2016.
- [3] Department of Energy, US, "Benefits of Demand Response in Electricity Markets and Recommendations for Achieving them," US Washington, DC: Department of Energy, 2006. [Online]. Available: <http://eetd.lbl.gov/ea/EMP/reports/congress-1252d.pdf>.
- [4] N. OConnell, P. Pinson, H. Madsen, and M. OMalley, "Benefits and challenges of electrical demand response: A critical review," *Renewable and Sustainable Energy Reviews*, vol. 39, pp. 686–699, 2014.
- [5] X. Yan, Y. Ozturk, Z. Hu, and Y. Song, "A review on price-driven residential demand response," *Renewable and Sustainable Energy Reviews*, vol. 96, pp. 411–419, 2018.
- [6] Q. Hu, F. Li, X. Fang, and L. Bai, "A framework of residential demand aggregation with financial incentives," *IEEE Transactions on Smart Grid*, vol. 9, no. 1, pp. 497–505, Jan. 2018.
- [7] P. Paudyal, P. Munankarmi, Z. Ni, and T. M. Hansen, "Incentive-based residential energy optimization considering comfort and voltage impacts," in *2018 IEEE Power Energy Society General Meeting (PESGM)*, Aug. 5 pages, 2018. DOI: 10.1109/PESGM.2018.8585827.
- [8] M. Albadi and E. El-Saadany, "A summary of demand response in electricity markets," *Electric Power Systems Research*, vol. 78, no. 11, 1989–1996, 2008.
- [9] K. M. Tsui and S. C. Chan, "Demand response optimization for smart home scheduling under real-time pricing," *IEEE Transactions on Smart Grid*, vol. 3, no. 4, pp. 1812–1821, Dec. 2012.
- [10] C. O. Adika and L. Wang, "Autonomous appliance scheduling for household energy management," *IEEE Transactions on Smart Grid*, vol. 5, no. 2, pp. 673–682, Mar. 2014.
- [11] F. A. Qayyum, M. Naeem, A. S. Khwaja, A. Anpalagan, L. Guan, and B. Venkatesh, "Appliance scheduling optimization in smart home networks," *IEEE Access*, vol. 3, pp. 2176–2190, 2015.

- [12] A. Agnetis, G. de Pascale, P. Detti, and A. Vicino, "Load scheduling for household energy consumption optimization," *IEEE Transactions on Smart Grid*, vol. 4, no. 4, pp. 2364–2373, Dec. 2013.
- [13] M. Beaudin, H. Zareipour, A. K. Bejestani, and A. Schellenberg, "Residential energy management using a two-horizon algorithm," *IEEE Transactions on Smart Grid*, vol. 5, no. 4, pp. 1712–1723, Jul. 2014.
- [14] T. M. Hansen, E. K. P. Chong, S. Suryanarayanan, A. A. Maciejewski, and H. J. Siegel, "A partially observable markov decision process approach to residential home energy management," *IEEE Transactions on Smart Grid*, vol. 9, no. 2, pp. 1271–1281, Mar. 2018.
- [15] Z. Zhao, W. C. Lee, Y. Shin, and K. Song, "An optimal power scheduling method for demand response in home energy management system," *IEEE Transactions on Smart Grid*, vol. 4, no. 3, pp. 1391–1400, Sep. 2013.
- [16] N. Javaid, M. Naseem, M. B. Rasheed, D. Mahmood, S. A. Khan, N. Alrajeh, and Z. Iqbal, "A new heuristically optimized home energy management controller for smart grid," *Sustainable Cities and Society*, vol. 34, pp. 211–227, 2017.
- [17] M. S. Ahmed, A. Mohamed, T. Khatib, H. Shareef, R. Z. Homod, and J. A. Ali, "Real time optimal schedule controller for home energy management system using new binary backtracking search algorithm," *Energy and Buildings*, vol. 138, pp. 215–227, 2017.
- [18] Y. Zhou, Y. Chen, G. Xu, Q. Zhang, and L. Krundel, "Home energy management with pso in smart grid," in *2014 IEEE 23rd International Symposium on Industrial Electronics (ISIE)*, Jun. 2014, pp. 1666–1670.
- [19] M. B. Rasheed, N. Javaid, A. Ahmad, Z. A. Khan, U. Qasim, and N. Alrajeh, "An efficient power scheduling scheme for residential load management in smart homes," *Applied Sciences*, vol. 5, no. 4, pp. 1134–1163, 2015.
- [20] J. H. Yoon, R. Baldick, and A. Novoselac, "Dynamic demand response controller based on real-time retail price for residential buildings," *IEEE Transactions on Smart Grid*, vol. 5, no. 1, pp. 121–129, Jan. 2014.
- [21] C. Corbin and G. Henze, "Predictive control of residential hvac and its impact on the grid. part i: Simulation framework and models," *Journal of Building Performance Simulation*, vol. 10, no. 3, pp. 294–312, 2017.
- [22] R. Godina, E. Rodrigues, E. Pouresmaeil, J. Matias, and J. Catalão, "Model predictive control home energy management and optimization strategy with demand response," *Applied Sciences*, vol. 8, no. 3, p. 408, 2018.
- [23] C. Chen, J. Wang, and S. Kishore, "A distributed direct load control approach for large-scale residential demand response," *IEEE Transactions on Power Systems*, vol. 29, no. 5, pp. 2219–2228, Sep. 2014.

- [24] J. Ning, Y. Tang, Q. Chen, J. Wang, J. Zhou, and B. Gao, "A bi-level coordinated optimization strategy for smart appliances considering online demand response potential," *Energies*, vol. 10, no. 4, 16 pages, 2017.
- [25] T. M. Hansen, R. Roche, S. Suryanarayanan, A. A. Maciejewski, and H. J. Siegel, "Heuristic optimization for an aggregator-based resource allocation in the Smart Grid," *IEEE Transactions on Smart Grid*, vol. 6, no. 4, pp. 1785–1794, July 2015.
- [26] Q. Hu, F. Li, X. Fang, and L. Bai, "A framework of residential demand aggregation with financial incentives," *IEEE Transactions on Smart Grid*, vol. 9, no. 1, pp. 497–505, Jan. 2018.
- [27] U.S. Department of Energy, "Use of electricity - energy explained, your guide to understanding energy - energy information administration," Accessed: Mar. 10, 2017. [Online]. Available: http://www.eia.gov/energyexplained/index.cfm?page=electricity_use.
- [28] D. B. Crawley, L. K. Lawrie, F. C. Winkelmann, W. F. Buhl, Y. J. Huang, C. O. Pedersen, R. K. Strand, R. J. Liesen, D. E. Fisher, M. J. Witte, and J. Glazer, "EnergyPlus: Creating a new-generation building energy simulation program," *Energy and Buildings*, vol. 33, no. 4, pp. 319–331, Apr. 2001.
- [29] D. P. Chassin, K. Schneider, and C. Gerkenmeyer, "GridLAB-D: An open-source power systems modeling and simulation environment," in *IEEE PES Transmission and Distribution Conference and Exposition*, Apr. 2008, 5 pp.
- [30] T. M. Hansen, R. Kadavil, B. Palmintier, S. Suryanarayanan, A. A. Maciejewski, H. J. Siegel, E. K. P. Chong, and E. Hale, "Enabling Smart Grid co-simulation studies," *IEEE Electrification*, vol. 4, no. 1, pp. 25–32, Mar. 2016.
- [31] R. Roche, S. Natarajan, A. Bhattacharyya, and S. Suryanarayanan, "A framework for co-simulation of ai tools with power system analysis software," in *23rd International Workshop on Database and Expert Systems Applications (DEXA)*, Sep. 2012, pp. 350–354.
- [32] T. M. Hansen, B. Palmintier, S. Suryanarayanan, A. A. Maciejewski, and H. J. Siegel, "Bus.py: A GridLAB-D communication interface for smart distribution grid simulations," in *IEEE Power and Energy Society General Meeting 2015*, 5 pages, July 2015.
- [33] M. Wetter, "Co-simulation of building energy and control systems with the building controls virtual test bed," *Journal of Building Performance Simulation*, vol. 4, no. 3, pp. 185–203, 2011.
- [34] W. Bernal, M. Behl, T. X. Nghiem, and R. Mangharam, "Mle+: A tool for integrated design and deployment of energy efficient building controls," in *Proceedings of the Fourth ACM Workshop on Embedded Sensing Systems for Energy-Efficiency in Buildings*, ACM, 2012, pp. 123–130.

- [35] PNNL, “Transactive energy simulation platform (TESP),” Accessed: Aug. 07, 2017. [Online]. Available: <http://tesp.readthedocs.io/en/latest/>.
- [36] S. Ciraci, J. Daily, J. Fuller, A. Fisher, L. Marinovici, and K. Agarwal, “FnCS: A framework for power system and communication networks co-simulation,” in *Proceedings of the Symposium on Theory of Modeling & Simulation - DEVS Integrative*, ser. DEVS 14, San Diego, CA, USA: Society for Computer Simulation International, 2014, 36:1–36:8.
- [37] Z. T. Taylor, K. Gowri, and S. Katipamula, “Gridlab-d technical support document: Residential end-use module version 1.0,” Pacific Northwest National Laboratory, Richland, WA, Tech. Rep., 2008.
- [38] C. Christensen, R. Anderson, S. Horowitz, A. Courtney, and J. Spencer, “Beopt software for building energy optimization: Features and capabilities,” National Renewable Energy Laboratory, Tech. Rep. NREL/TP-550-39929, 2006.
- [39] R. Hendron and C. Engebrecht, “Building America research benchmark definition,” National Renewable Energy Laboratory, Tech. Rep. NREL/TP-550-47246, Jan. 2010.
- [40] R. Tonkoski, L. Lopes, and T. El-Fouly, “Coordinated active power curtailment of grid connected PV inverters for overvoltage prevention,” *IEEE Transactions on Sustainable Energy*, vol. 2, no. 2, pp. 139–147, 2011.
- [41] S. Mittal, M. Ruth, A. Pratt, M. Lunacek, D. Krishnamurthy, and W. Jones, “A system-of-systems approach for integrated energy systems modeling and simulation,” in *Proceeding of the conference on summer computer simulation*, 2015, 10 pp.
- [42] J. Tan and L. Wang, “Integration of plug-in hybrid electric vehicles into residential distribution grid based on two-layer intelligent optimization,” *IEEE Transactions on Smart Grid*, vol. 5, no. 4, pp. 1774–1784, 2014.
- [43] ENERGY STAR, “A Guide to Energy-Efficient Heating and Cooling,” 2009. [Online]. Available: http://www.energystar.gov/ia/partners/publications/pubdocs/HeatingCoolingGuide%20FINAL_9-4-09.pdf.
- [44] W. E. Hart, J.-P. Watson, and D. L. Woodruff, “Pyomo: Modeling and solving mathematical programs in Python,” *Mathematical Programming Computation*, vol. 3, no. 3, pp. 219–260, 2011.
- [45] ComEd, “ComEd hourly pricing program,” Accessed: Mar. 20, 2017. [Online]. Available: <http://hourlypricing.comed.com/live-prices/>.
- [46] Z. Chen, L. Wu, and Y. Fu, “Real-time price-based demand response management for residential appliances via stochastic optimization and robust optimization,” *IEEE Transactions on Smart Grid*, vol. 3, no. 4, pp. 1822–1831, Dec. 2012.

- [47] D. T. Nguyen and L. B. Le, "Joint optimization of electric vehicle and home energy scheduling considering user comfort preference," *IEEE Transactions on Smart Grid*, vol. 5, no. 1, pp. 188–199, Jan. 2014.
- [48] M. Muratori and G. Rizzoni, "Residential demand response: Dynamic energy management and time-varying electricity pricing," *IEEE Transactions on Power Systems*, vol. 31, no. 2, pp. 1108–1117, Mar. 2016.
- [49] Y. Huang, L. Wang, W. Guo, Q. Kang, and Q. Wu, "Chance constrained optimization in a home energy management system," *IEEE Transactions on Smart Grid*, vol. 9, no. 1, pp. 252–260, Jan. 2018.
- [50] Z. Yu, L. Jia, M. C. Murphy-Hoye, A. Pratt, and L. Tong, "Modeling and stochastic control for home energy management," *IEEE Transactions on Smart Grid*, vol. 4, no. 4, pp. 2244–2255, Dec. 2013.
- [51] P. Samadi, H. Mohsenian-Rad, V. W. S. Wong, and R. Schober, "Tackling the load uncertainty challenges for energy consumption scheduling in smart grid," *IEEE Transactions on Smart Grid*, vol. 4, no. 2, pp. 1007–1016, Jun. 2013.
- [52] E. Wilson, C. Engebrecht-Metzger, S. Horowitz, and R. Hendron, "2014 building america house simulation protocols," National Renewable Energy Laboratory, Tech. Rep. NREL/TP-5500-60988, Mar. 2014.
- [53] R. Godina, E. M. G. Rodrigues, E. Pouresmaeil, J. C. O. Matias, and J. P. S. Catalão, "Model predictive control technique for energy optimization in residential sector," in *2016 IEEE 16th International Conference on Environment and Electrical Engineering (EEEIC)*, Jun. 6 pages, 2016.
- [54] M. R. Sarker, M. A. Ortega-Vazquez, and D. S. Kirschen, "Optimal coordination and scheduling of demand response via monetary incentives," *IEEE Transactions on Smart Grid*, vol. 6, no. 3, pp. 1341–1352, May 2015.
- [55] S. U. Agamah and L. Ekonomou, "A heuristic combinatorial optimization algorithm for load-leveling and peak demand reduction using energy storage systems," *Electric Power Components and Systems*, vol. 45, no. 19, pp. 2093–2103, 2017.
- [56] A. Das and Z. Ni, "A computationally efficient optimization approach for battery systems in islanded microgrid," *IEEE Transactions on Smart Grid*, 11 pages, 2017, in press. DOI: 10.1109/TSG.2017.2713947.
- [57] J. Gao, "Machine learning applications for data center optimization," Google White Paper, 2014.
- [58] E. Mocanu, D. C. Mocanu, P. H. Nguyen, A. Liotta, M. E. Webber, M. Gibescu, and J. G. Slootweg, "On-line building energy optimization using deep reinforcement learning," *IEEE Transactions on Smart Grid*, 9 pages, 2018, in press. DOI: 10.1109/TSG.2018.2834219.

- [59] Y. Zhang, N. Rahbari-Asr, J. Duan, and M. Chow, "Day-ahead smart grid cooperative distributed energy scheduling with renewable and storage integration," *IEEE Transactions on Sustainable Energy*, vol. 7, no. 4, pp. 1739–1748, Oct. 2016.
- [60] S. Park, J. Lee, S. Bae, G. Hwang, and J. K. Choi, "Contribution-based energy-trading mechanism in microgrids for future smart grid: A game theoretic approach," *IEEE Transactions on Industrial Electronics*, vol. 63, no. 7, pp. 4255–4265, 2016.
- [61] M. Liu, Y. Shi, and X. Liu, "Distributed mpc of aggregated heterogeneous thermostatically controlled loads in smart grid," *IEEE Transactions on Industrial Electronics*, vol. 63, no. 2, pp. 1120–1129, Feb. 2016.
- [62] N. Liu, X. Yu, C. Wang, and J. Wang, "Energy sharing management for microgrids with pv prosumers: A stackelberg game approach," *IEEE Transactions on Industrial Informatics*, vol. 13, no. 3, pp. 1088–1098, Jun. 2017.
- [63] A. Ouammi, H. Dagdougui, L. Dessaint, and R. Sacile, "Coordinated model predictive-based power flows control in a cooperative network of smart microgrids," *IEEE Transactions on Smart Grid*, vol. 6, no. 5, pp. 2233–2244, Sep. 2015.
- [64] A. Parisio, C. Wiezorek, T. Kyntäjä, J. Elo, K. Strunz, and K. H. Johansson, "Cooperative mpc-based energy management for networked microgrids," *IEEE Transactions on Smart Grid*, vol. 8, no. 6, pp. 3066–3074, Nov. 2017.
- [65] R. Halvgaard, L. Vandenberghe, N. K. Poulsen, H. Madsen, and J. B. Jørgensen, "Distributed model predictive control for smart energy systems," *IEEE Transactions on Smart Grid*, vol. 7, no. 3, pp. 1675–1682, May 2016.
- [66] Z. Wang, B. Chen, J. Wang, M. M. Begovic, and C. Chen, "Coordinated energy management of networked microgrids in distribution systems," *IEEE Transactions on Smart Grid*, vol. 6, no. 1, pp. 45–53, Jan. 2015.
- [67] M. R. Sarker, M. A. Ortega-Vazquez, and D. S. Kirschen, "Optimal coordination and scheduling of demand response via monetary incentives," *IEEE Transactions on Smart Grid*, vol. 6, no. 3, pp. 1341–1352, May 2015.
- [68] J. Wang, M. Biviji, and W. M. Wang, "Case studies of smart grid demand response programs in north america," in *ISGT 2011*, Jan. 5 pages, 2011. DOI: 10.1109/ISGT.2011.5759162.
- [69] M. Mallette and G. Venkataramanan, "Financial incentives to encourage demand response participation by plug-in hybrid electric vehicle owners," in *2010 IEEE Energy Conversion Congress and Exposition*, Sep. 2010, pp. 4278–4284. DOI: 10.1109/ECCE.2010.5618472.

- [70] Z. Ni, P. Paudyal, and X. Zhong, "A computational intelligence approach for residential home energy management considering reward incentives," in *2017 IEEE Symposium Series on Computational Intelligence (SSCI)*, Nov. 8 pages, 2017. DOI: 10.1109/SSCI.2017.8285256.
- [71] N. Lu, "An evaluation of the HVAC load potential for providing load balancing service," *IEEE Transactions on Smart Grid*, vol. 3, no. 3, pp. 1263–1270, 2012.
- [72] J. Kondoh, N. Lu, and D. J. Hammerstrom, "An evaluation of the water heater load potential for providing regulation service," *IEEE Transactions on Power Systems*, vol. 26, no. 3, pp. 1309–1316, 2011.
- [73] K. Tomiyama, J. Daniel, and S. Ihara, "Modeling air conditioner load for power system studies," *IEEE Transactions on Power Systems*, vol. 13, no. 2, pp. 414–421, 1998.
- [74] J. C. Laurent and R. P. Malhame, "A physically-based computer model of aggregate electric water heating loads," *IEEE Transactions on Power Systems*, vol. 9, no. 3, pp. 1209–1217, Aug. 1994.
- [75] C. Alvarez, R. P. Malhame, and A. Gabaldon, "A class of models for load management application and evaluation revisited," *IEEE Transactions on Power Systems*, vol. 7, no. 4, pp. 1435–1443, Nov. 1992.
- [76] Z. Ni and A. Das, "A new incentive-based optimization scheme for residential community with financial trade-offs," *IEEE Access*, vol. 6, pp. 57 802–57 813, 2018.
- [77] S. Shao, M. Pipattanasomporn, and S. Rahman, "Development of physical-based demand response-enabled residential load models," *IEEE Transactions on Power Systems*, vol. 28, no. 2, pp. 607–614, 2013.
- [78] V. Durvasulu, T. M. Hansen, and R. Tonkoski, "Classification of Generators Participating in the Bulk-Power Market," in *18th IEEE International Conference on Industrial Technology (ICIT)*, Toronto, Ontario, Canada, Mar. 2017, pp. 575–579.
- [79] R. Billinton, S. Kumar, N. Chowdhury, K. Chu, K. Debnath, L. Goel, E. Khan, P. Kos, G. Nourbakhsh, and J. Oteng-Adjei, "A reliability test system for educational purposes-basic data," *IEEE Power Engineering Review*, vol. 9, no. 8, pp. 67–68, Aug. 1989.
- [80] United States Environmental Protection Agency, "Electricity customers," *EPA*, Mar. 2018, Accessed: June 10, 2018. [Online]. Available: <https://www.epa.gov/energy/electricity-customers>.
- [81] V. Durvasulu and T. M. Hansen, "Benefits of a demand response exchange participating in existing bulk-power markets," *Energies, special issue on Demand Response in Electricity Markets*, vol. 11, no. 12, 21 pages, Dec. 2018.

- [82] S. Sharma, V. Durvasulu, B. Celik, S. Suryanarayanan, Timothy M. Hansen, A. A. Maciejewski, and H. J. Siegel, “Metrics-Based Assessment of Sustainability in Demand Response,” in *15th IEEE International Conference on Smart City*, Bangkok, Thailand, pp. 130–137, Dec. 2017.
- [83] B. Hendron, J. Burch, and G. Barker, “Tool for generating realistic residential hot water event schedules,” in *Proceedings of SimBuild*, vol. 4, 2010, pp. 328–335.
- [84] PJM, “PJM-energy market,” *EPA*, Accessed: Mar. 14, 2018. [Online]. Available: <http://www.pjm.com/markets-and-operations/energy.aspx>.
- [85] PG&E, “Learn more about capacity bidding program,” Accessed: June 20, 2018. [Online]. Available: https://www.pge.com/en_US/business/save-energy-money/energy-management-programs/third-party-programs/capacity-bidding.page/.
- [86] SCE, “Capacity bidding program (cbp) aggregators,” Accessed: June 20, 2018. [Online]. Available: <https://www.sce.com/wps/portal/home/business/savings-incentives/demand-response/demand-responces-aggregator/>.